

Intercellular signaling and synaptic deconstruction uncovered by single-cell and spatial transcriptomics in an AD tauopathy model

Jeff X. Ji, Brian L. Giles, Surjyadipta Bhattacharjee, Marie-Audrey I. Kautzmann, Alisdair P. Masson, Sonia Do Carmo, A. Claudio Cuello, Nicolas G. Bazan

*Corresponding author: Nicolas G. Bazan
Email: nbazan@lsuhsc.edu

This PDF file includes:

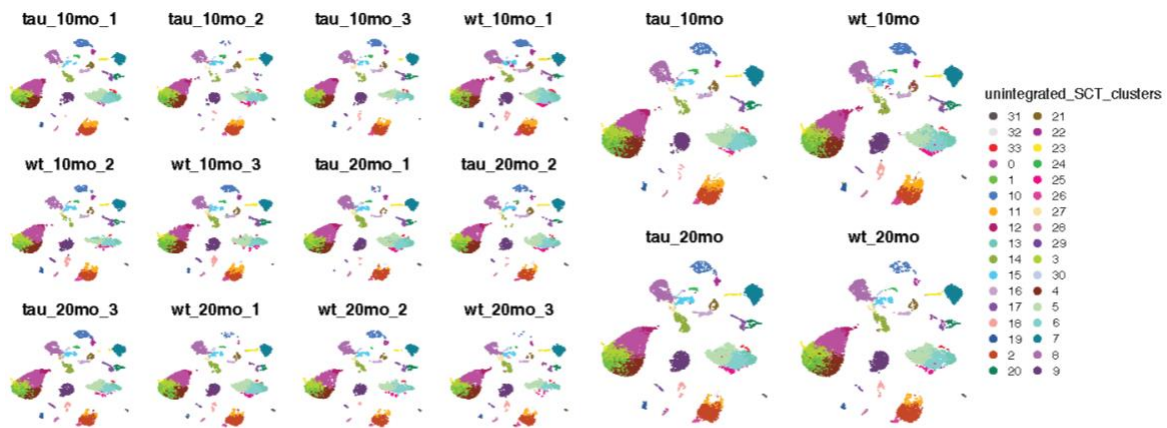
Supplementary Figures 1 to 30
Supplementary Tables 1 to 2
Legends for Supplementary Datasets 1 to 6

Other supporting materials for this manuscript include the following:

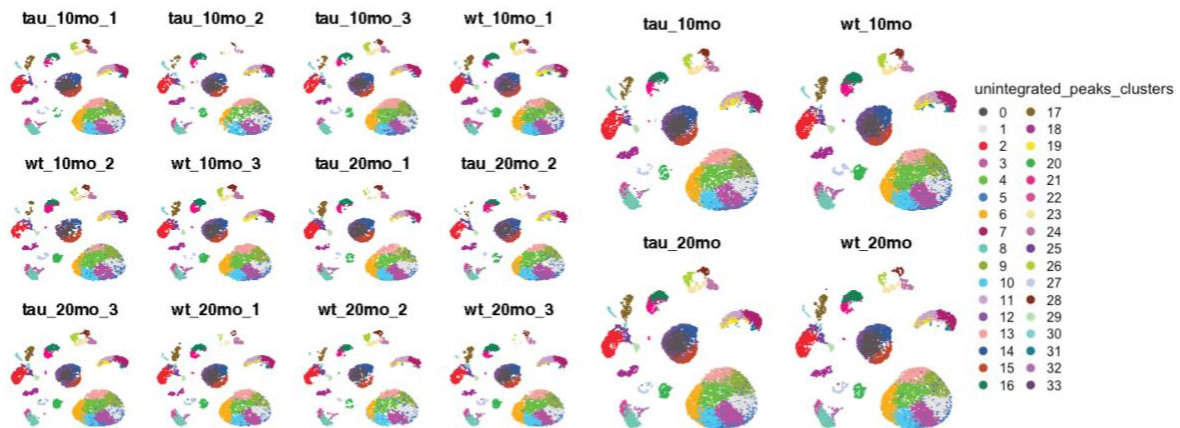
Supplementary Datasets 1 to 6

Supplementary Figures

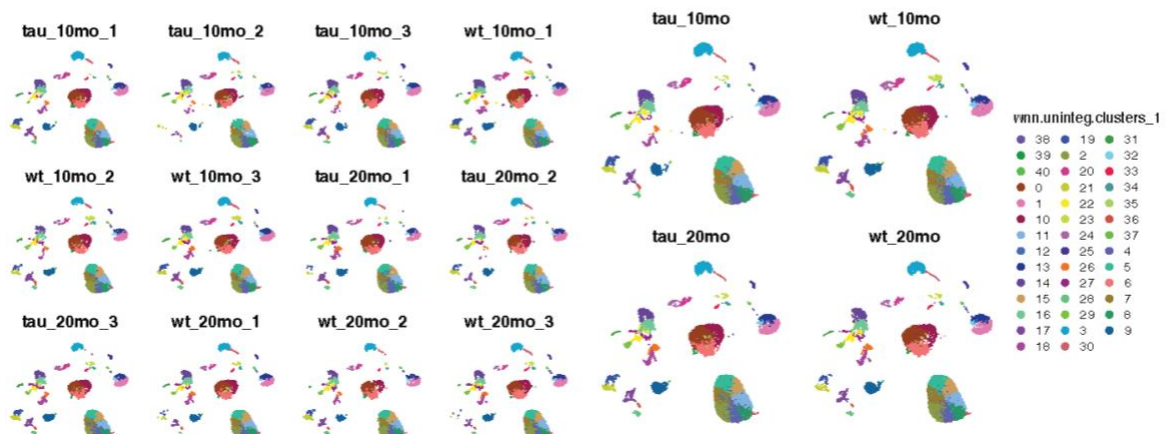
a



b

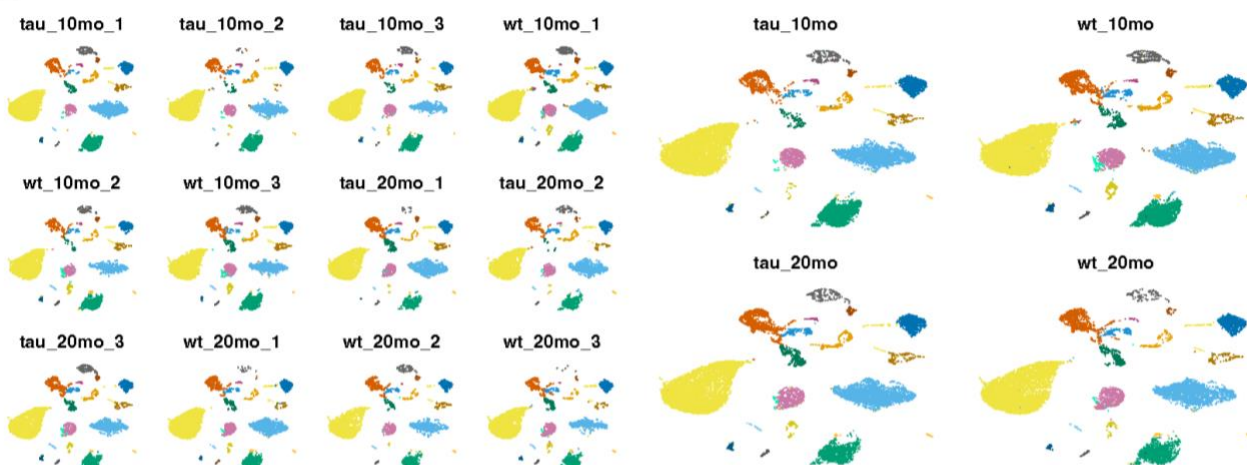


c

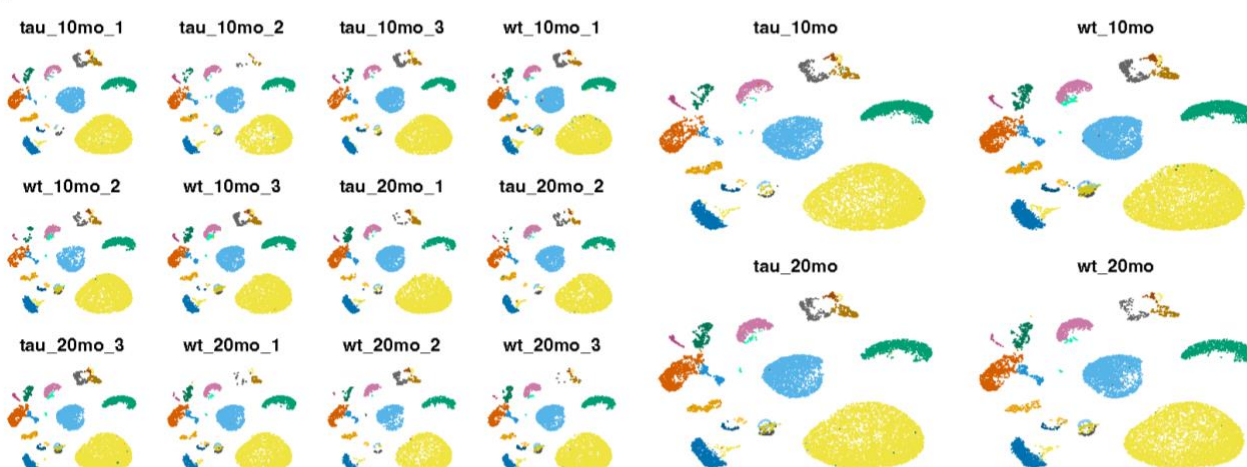


Supplementary Figure 1. Seurat clustering for (a) RNA, (b) ATAC, and (c) Weighted Nearest Neighbor (WNN). UMAPs for each individual sample (left) and combined with similar biological replicates (right). Unbiased clustering identified 34 unique clusters from snRNA (SCT normalized), 34 clusters from snATAC, and 41 clusters using WNN (combined snRNA and snATAC).

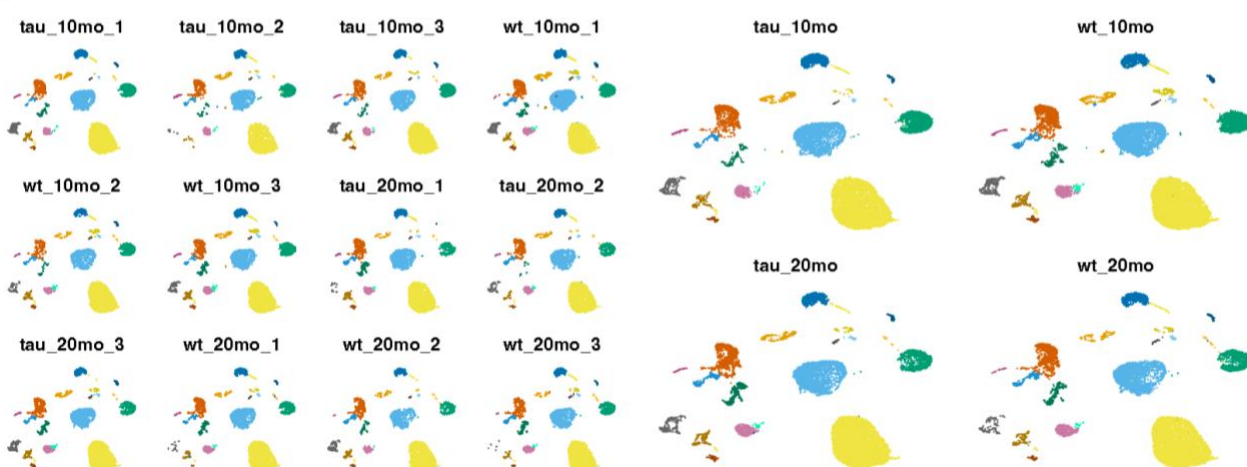
a



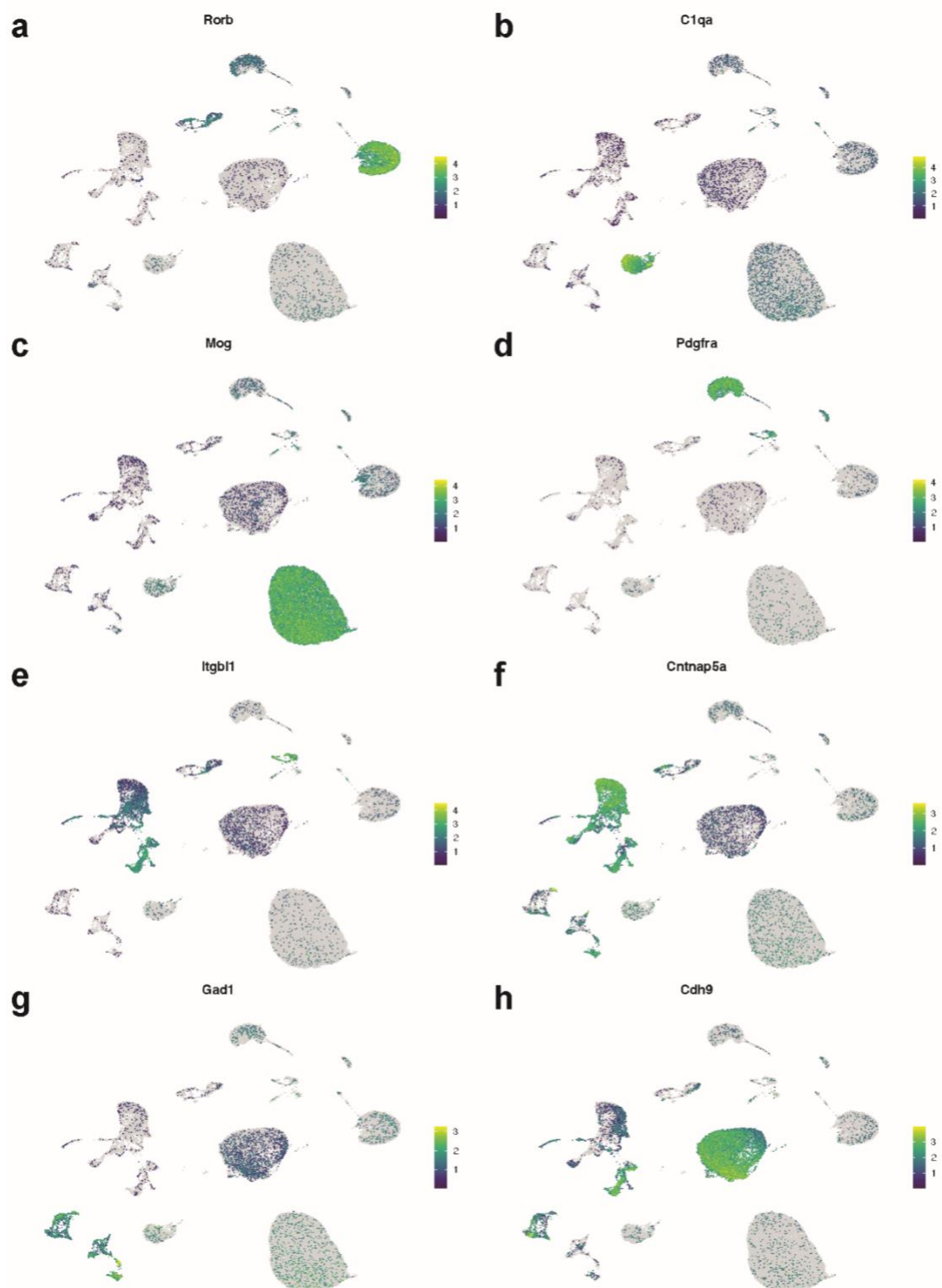
b



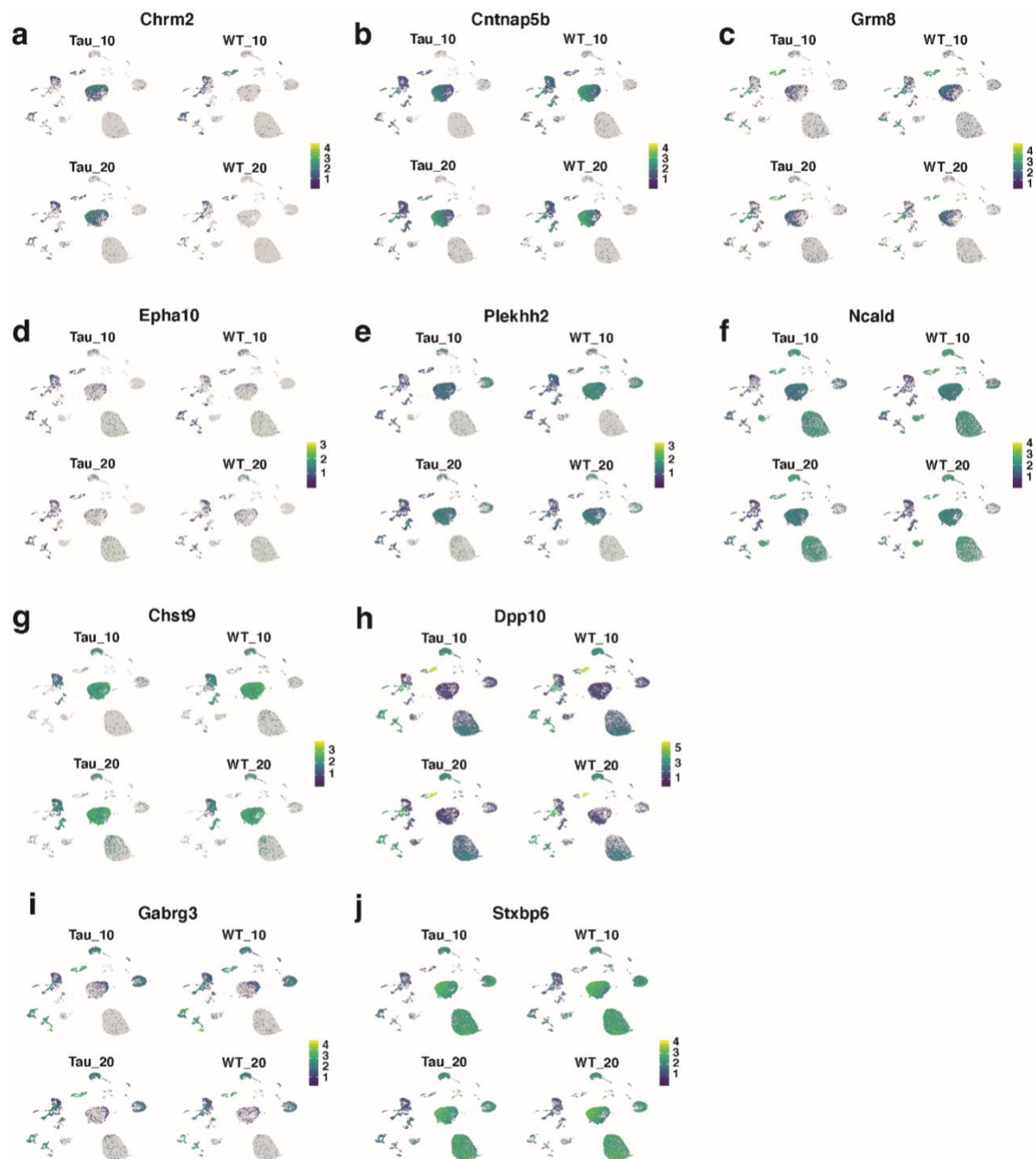
c



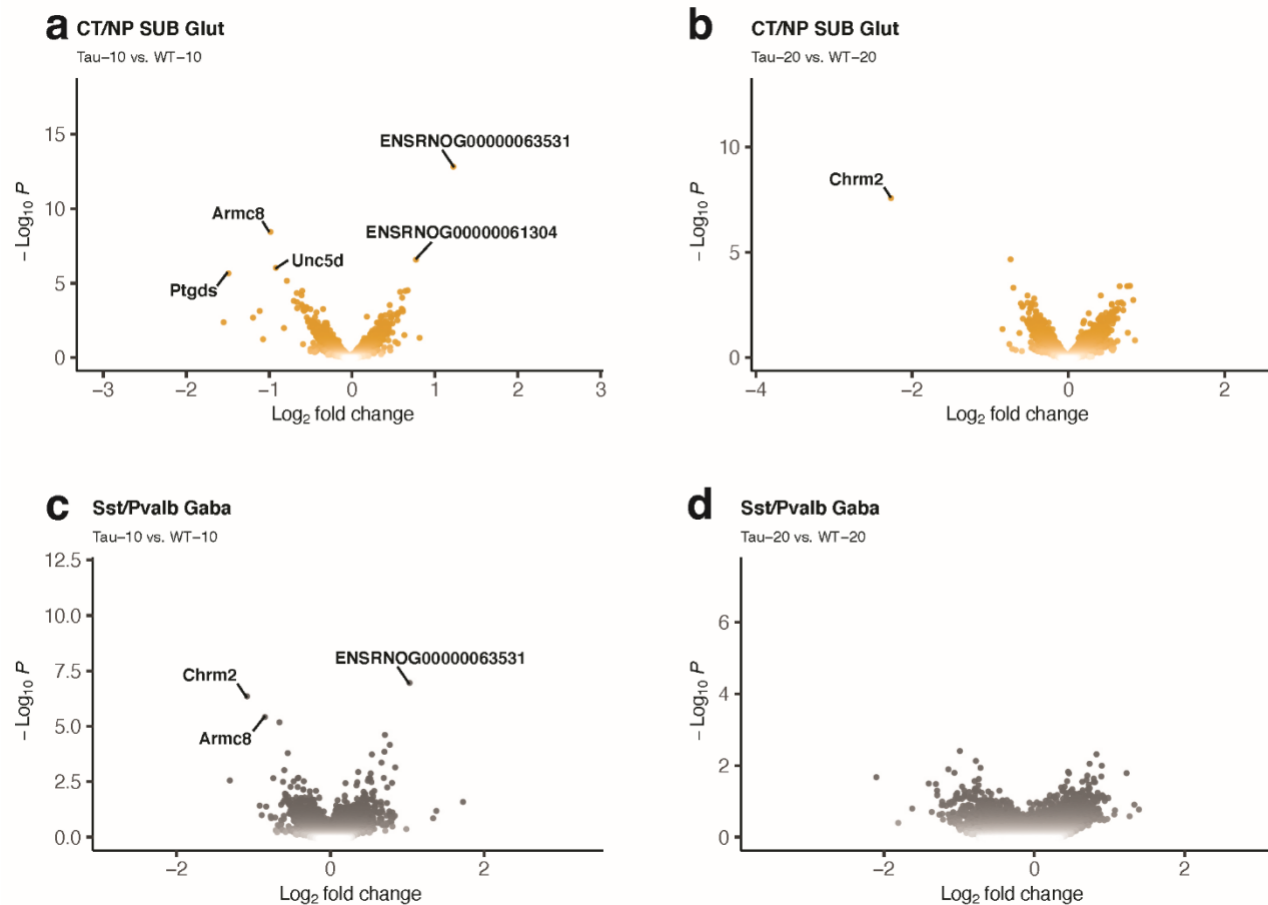
Supplementary Figure 2. Cell type identification for (a) RNA, (b) ATAC, and (c) WNN. UMAPs for each individual sample (left) and combined with similar biological replicates (right). Colors correspond to same labeling scheme throughout, highlighted in Figure 1A.



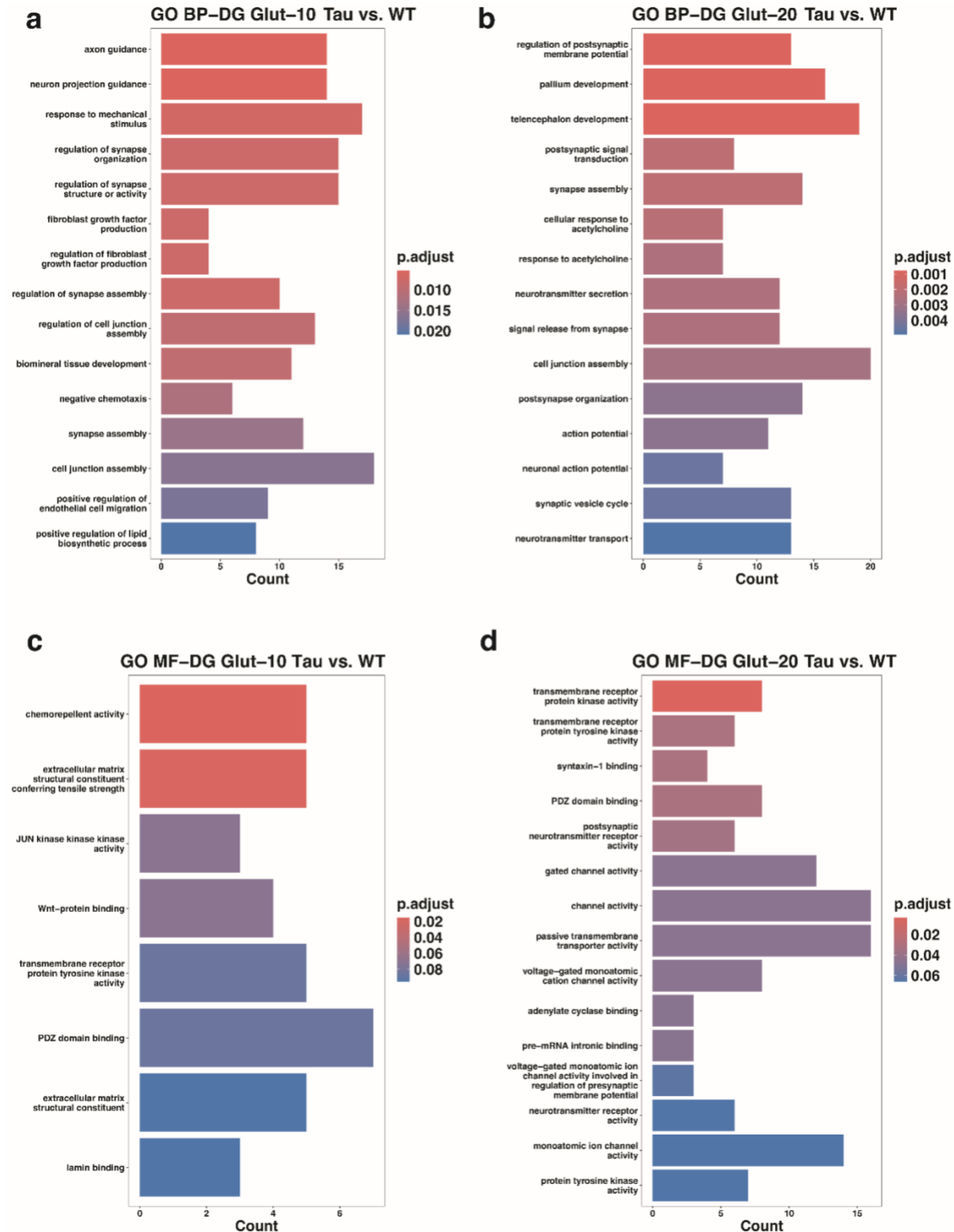
Supplementary Figure 3. Marker gene validation of cell type annotation. WNN dimensional reduction plots displaying the top marker gene for each cell type. Rorb expression for Astrocytes (**a**), C1qa expression for Microglia (**b**), Mog expression for Oligos (**c**), Pdgfra expression for OPCs (**d**), Itgb1 expression for CA3 (**e**), Cntnap5a expression for CA1 (**f**), Gad1 expression for GABAergic neurons (**g**), and Cdh9 for DG neurons (**h**).



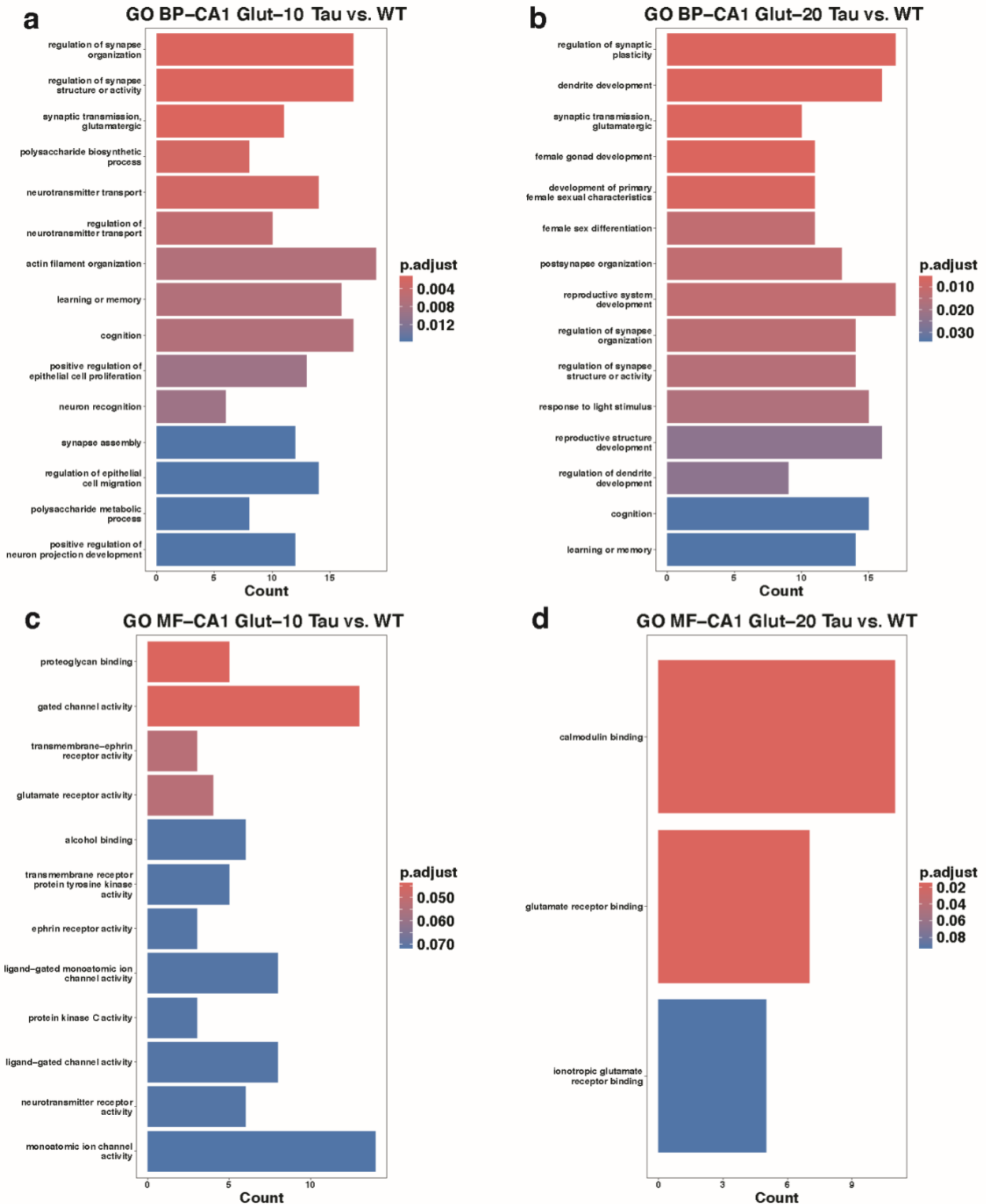
Supplementary Figure 4. Feature plot of the DEG highlighted in Figure 2D.



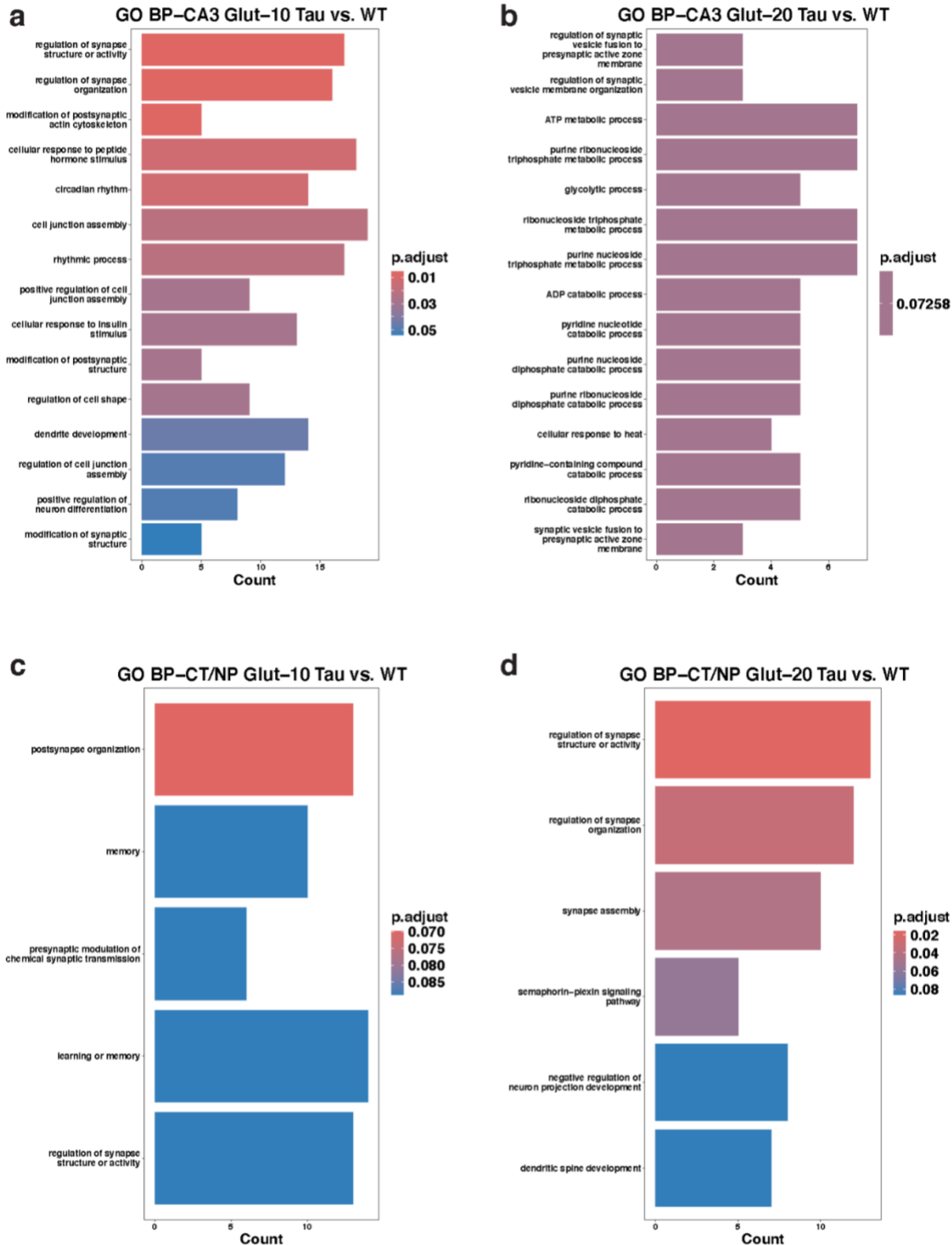
Supplementary Figure 5. Volcano plots showing DEG comparisons between Tau and WT at 10 and 20 months in CT/NP SUB Glut neurons (a,b) and Sst/Pvalb Gaba neurons (c,d). Labelled points satisfy the following criteria: p -adjusted values < 0.05 and $|\log_2 fc| > 0.15$.



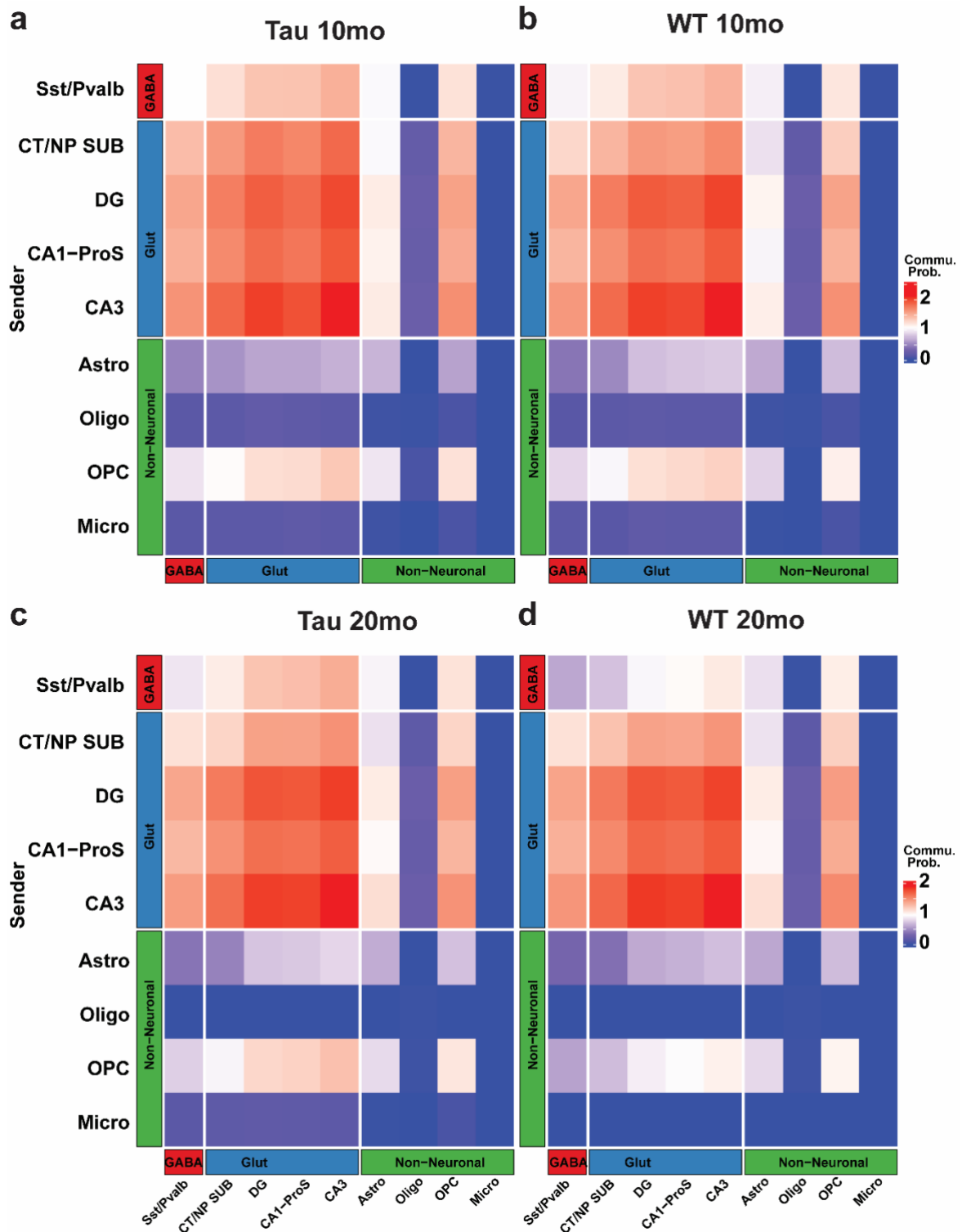
Supplementary Figure 6. Gene ontology (GO) pathway analysis of top DEG between Tau and WT in DG Glut neurons at 10 and 20 months. Up to 15 of the most significant pathways (p-adjusted <0.05) are shown. GO biological process (BP) between Tau and WT relate to synaptic organization, neurotransmitter release, and regulation of lipid synthesis (**a,b**). GO molecular functions (MF) revealed functions related to extracellular matrix structure, Wnt signaling, and various channel and receptor activity (**c,d**).



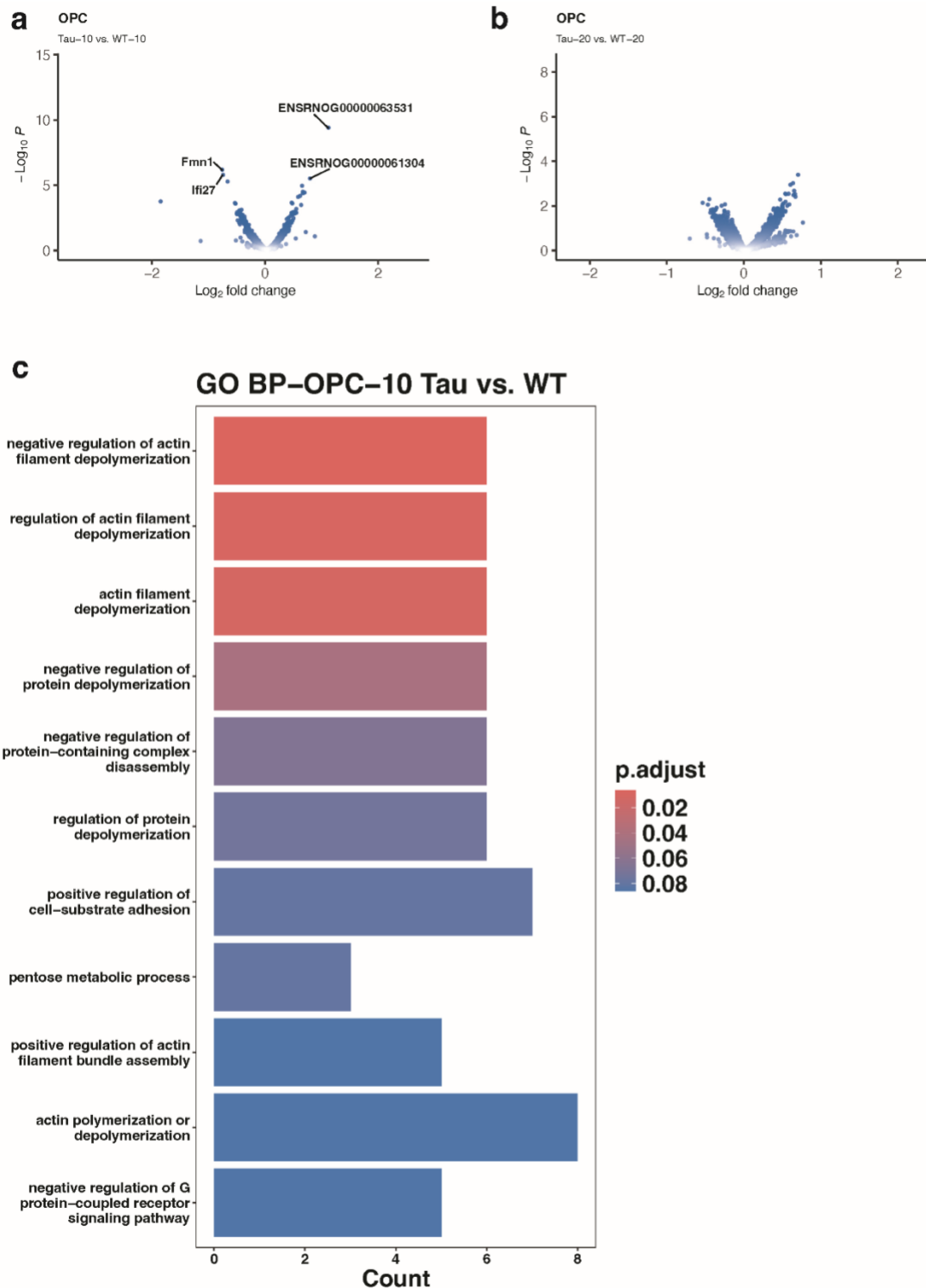
Supplementary Figure 7. Gene ontology (GO) pathway analysis of top DEG between Tau and WT in CA1 Glut neurons at 10 and 20 months. Up to 15 of the most significant pathways (p-adjusted <0.05) are shown. GO biological process (BP) between Tau and WT relate to synaptic organization, dendrite development, and glutamatergic transmission (**a,b**). GO molecular functions (MF) revealed functions related to synaptic receptor and channel activity, proteoglycan signaling, and calmodulin binding (**c,d**).



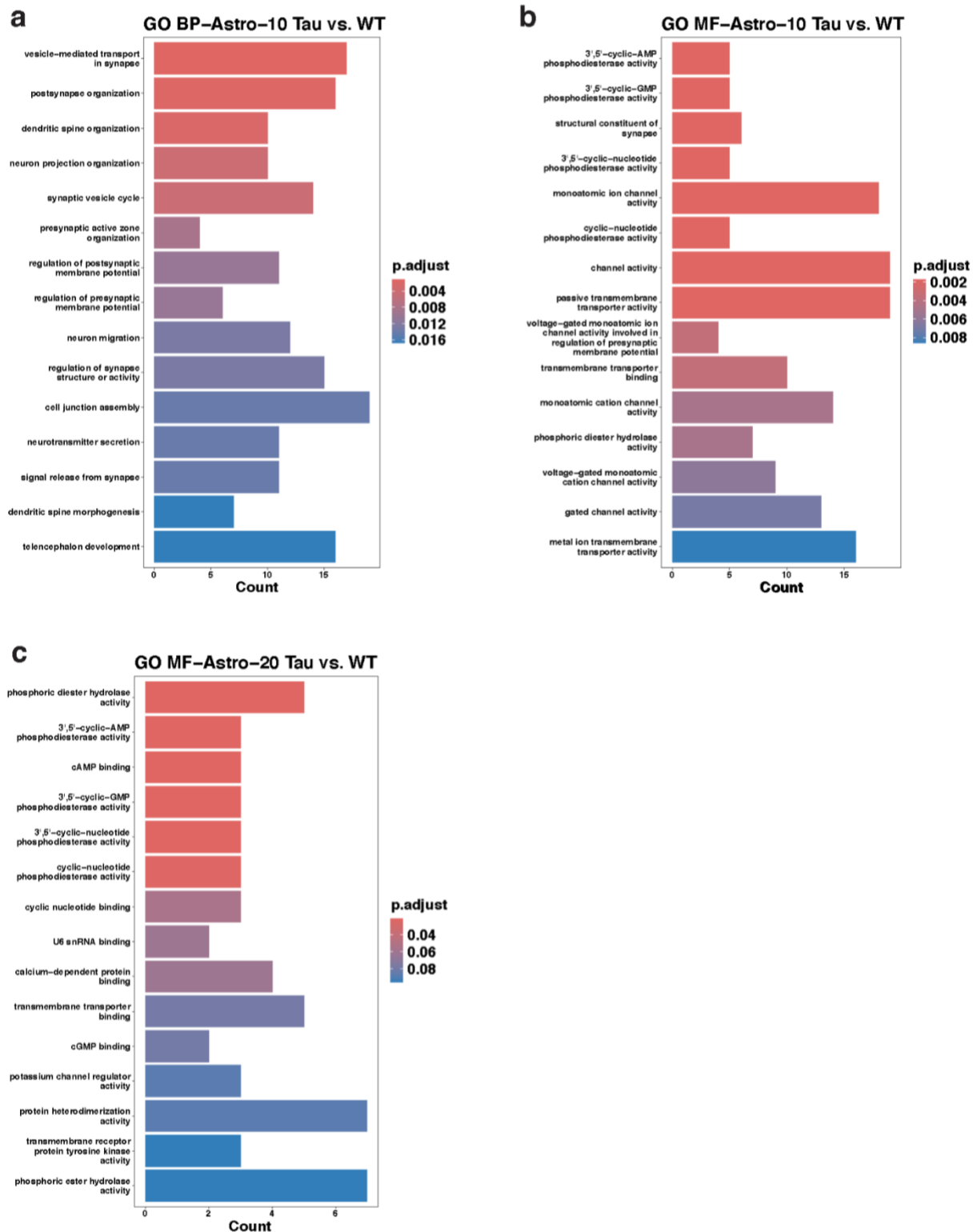
Supplementary Figure 8. Gene ontology (GO) pathway analysis of top DEG between Tau and WT in CA3 Glut neurons and CT/NP Glut neurons at 10 and 20 months. Up to 15 of the most significant pathways (p-adjusted <0.05) are shown. GO biological process (BP) between Tau and WT in CA3 Glut neurons relate to synaptic organization, cell junction assembly, and energy metabolism (**a,b**). GO BP in CT/NP Glut neurons relate to various synaptic activities (**c,d**).



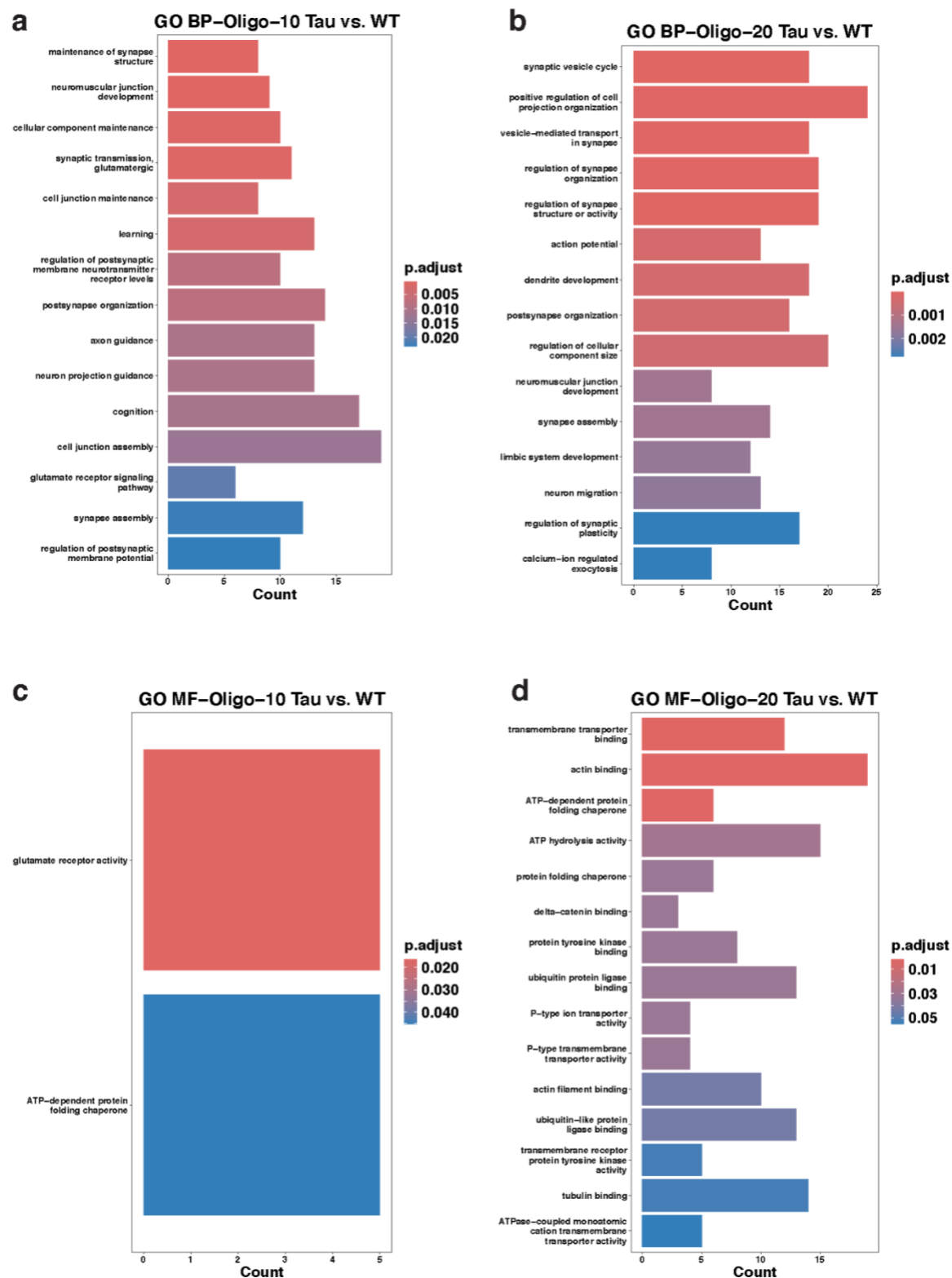
Supplementary Figure 9. Aggregated heatmap showing communication probabilities using the NeuronChat database in Tau 10-mo (a), WT 10-mo (b), Tau 20-mo (c), WT-20mo (d). The communication probability for cell pairs as senders or receivers are broken down into Glutamatergic neurons, GABAergic neurons, and non-neuronal cells, and the value of the intersection denotes the communication probability. In general, the strongest interactions occurred between DG, CA1-ProS, and CA3 Glutamatergic neurons.



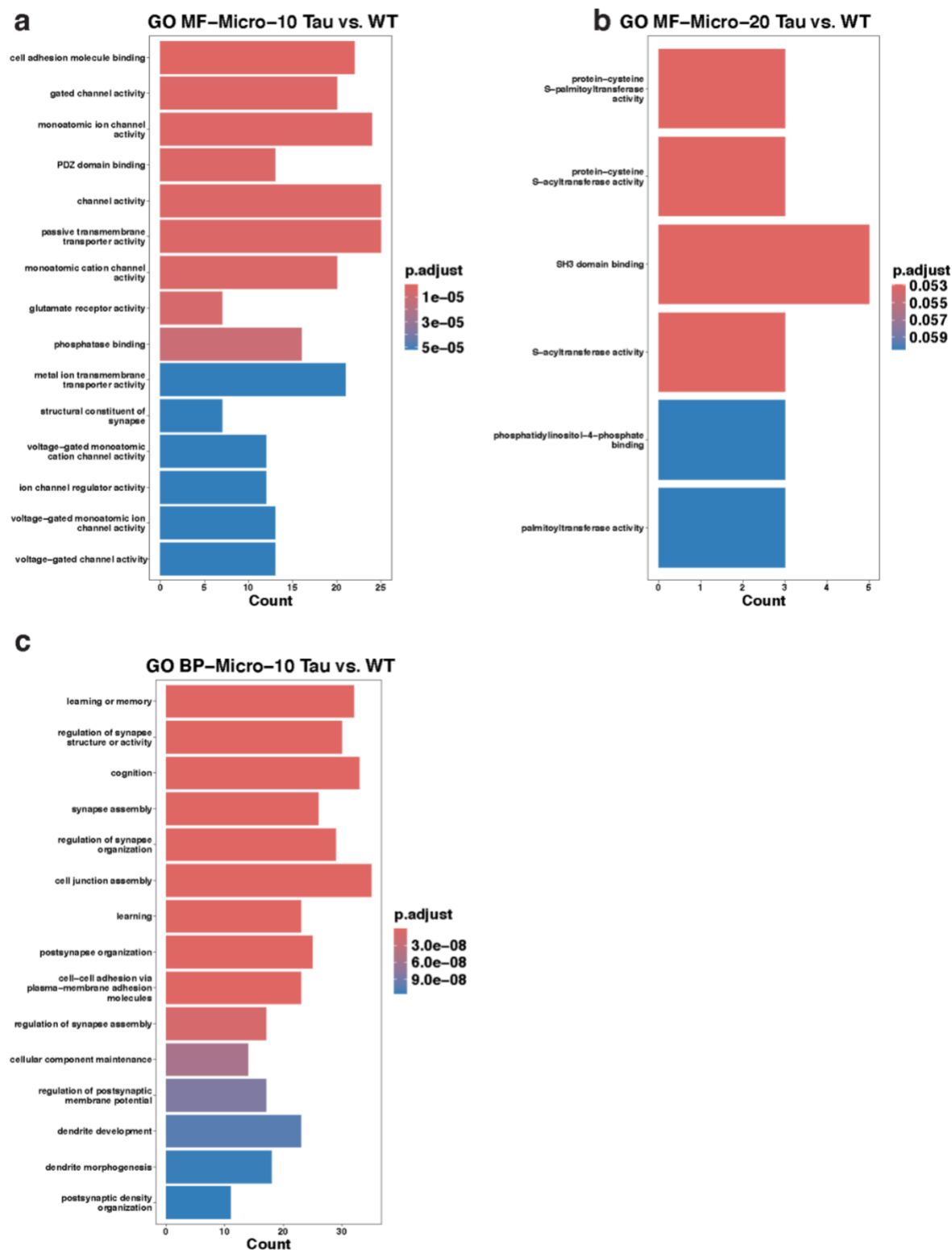
Supplementary Figure 10. Volcano plots showing DEG comparisons between Tau and WT at 10 (**a**) and 20 months (**b**) in OPC. Labelled points satisfy the following criteria: p-adjusted values < 0.05 and $|\log_2 \text{fc}| > 0.15$. (**c**) GO biological process (BP) pathways analysis of top DEG between Tau and WT in OPC at 10 months, related to cytoskeleton regulation through actin depolymerization. Up to 11 of the most significant pathways (p-adjusted < 0.05) are shown.



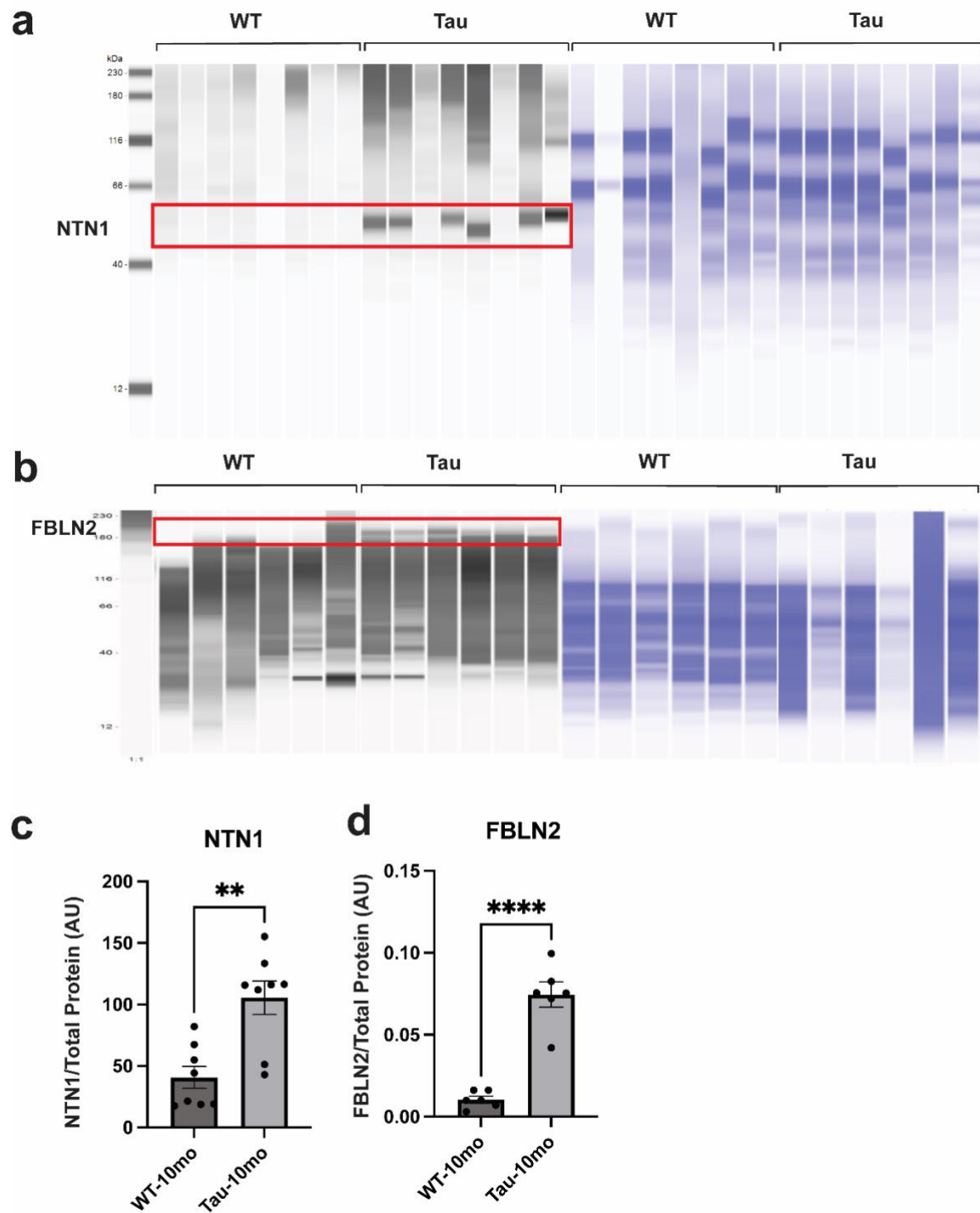
Supplementary Figure 11. GO BP (a) and MF (b,c) pathway analysis of top DEG between Tau and WT in Astrocytes at 10 and 20 months. Up to 15 of the most significant pathways (p-adjusted <0.05) are shown. GO BP between Tau and WT in Astrocytes at 10 months relate to synaptic organization and signal transduction (a). GO MF in Astrocytes at 10 and 20 months relate to channels activity at the synapse, signal transduction and various synaptic activities (b,c).



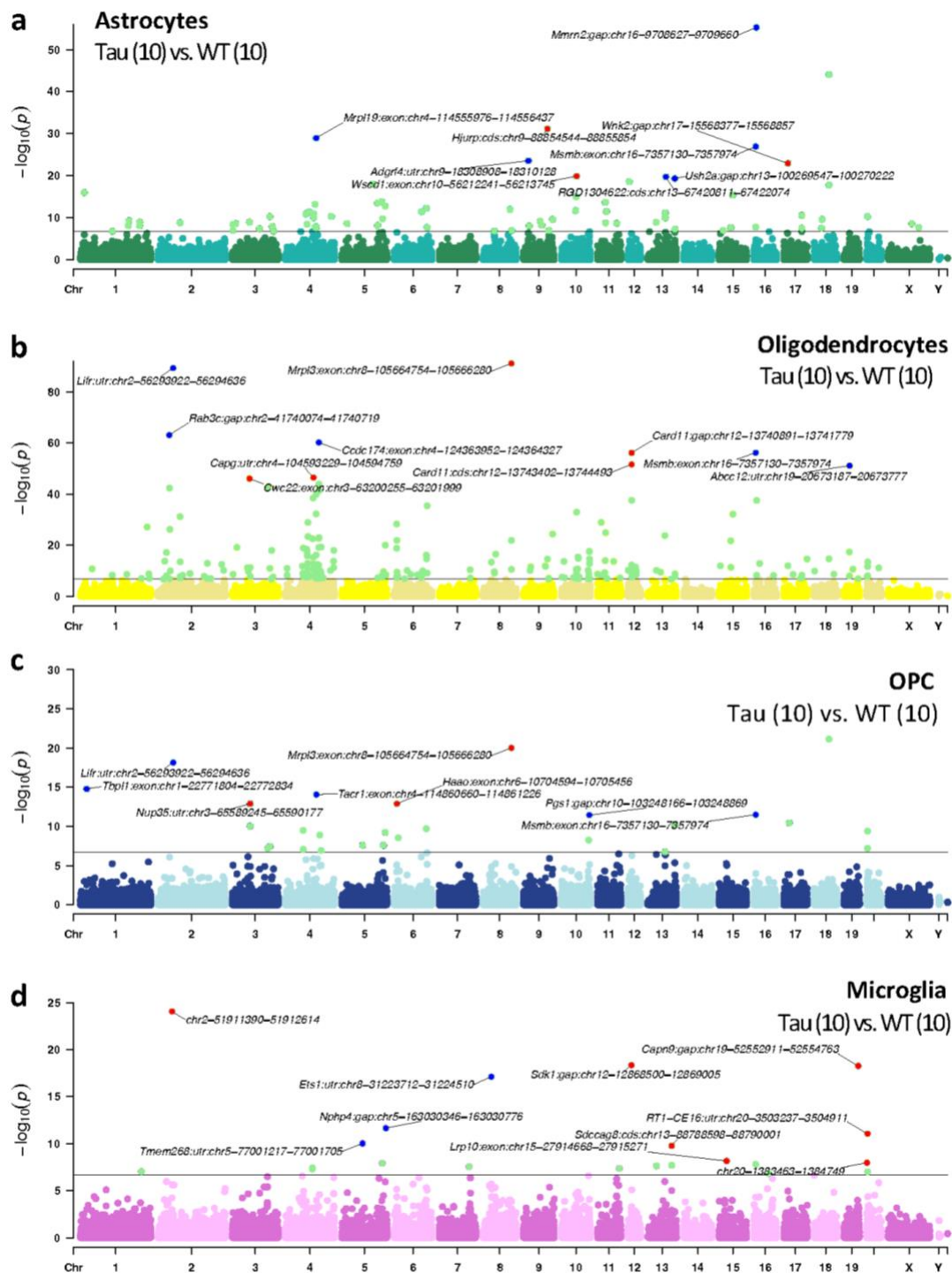
Supplementary Figure 12. GO BP (a,b) and MF (b,c) pathway analysis of top DEG between Tau and WT in Oligodendrocytes at 10 and 20 months. Up to 15 of the most significant pathways (p-adjusted <0.05) are shown (a,b,d). GO BP between Tau and WT in Oligodendrocytes at 10 and 20 months relates to synaptic organization, synapse assembly, synapse maintenance and neuronal migration (a,b). GO MF in Oligodendrocytes at 10 and 20 months relate to receptor activity and signal transduction (c,d).



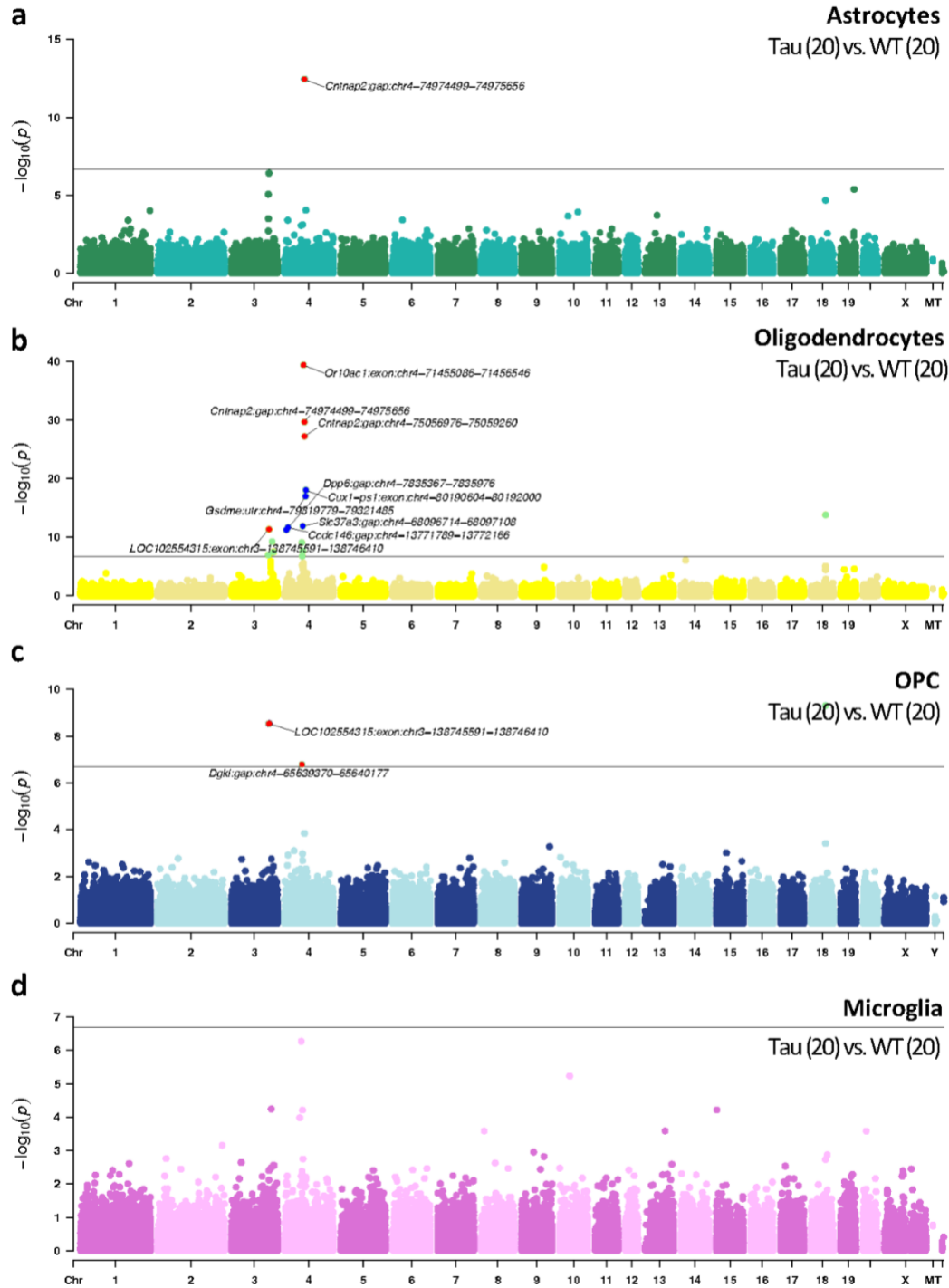
Supplementary Figure 13. GO MF (a,b) and BP (c) pathway analysis of top DEG between Tau and WT in Microglia at 10 and 20 months. Up to 15 of the most significant pathways (p-adjusted <0.05) are shown (a,c). GO MF between Tau and WT in Microglia at 10 and 20 months relate to channel activity (a) and signal transduction (b). GO BP in Microglia at 10 months relates to learning, cognition and various synaptic activities (c).



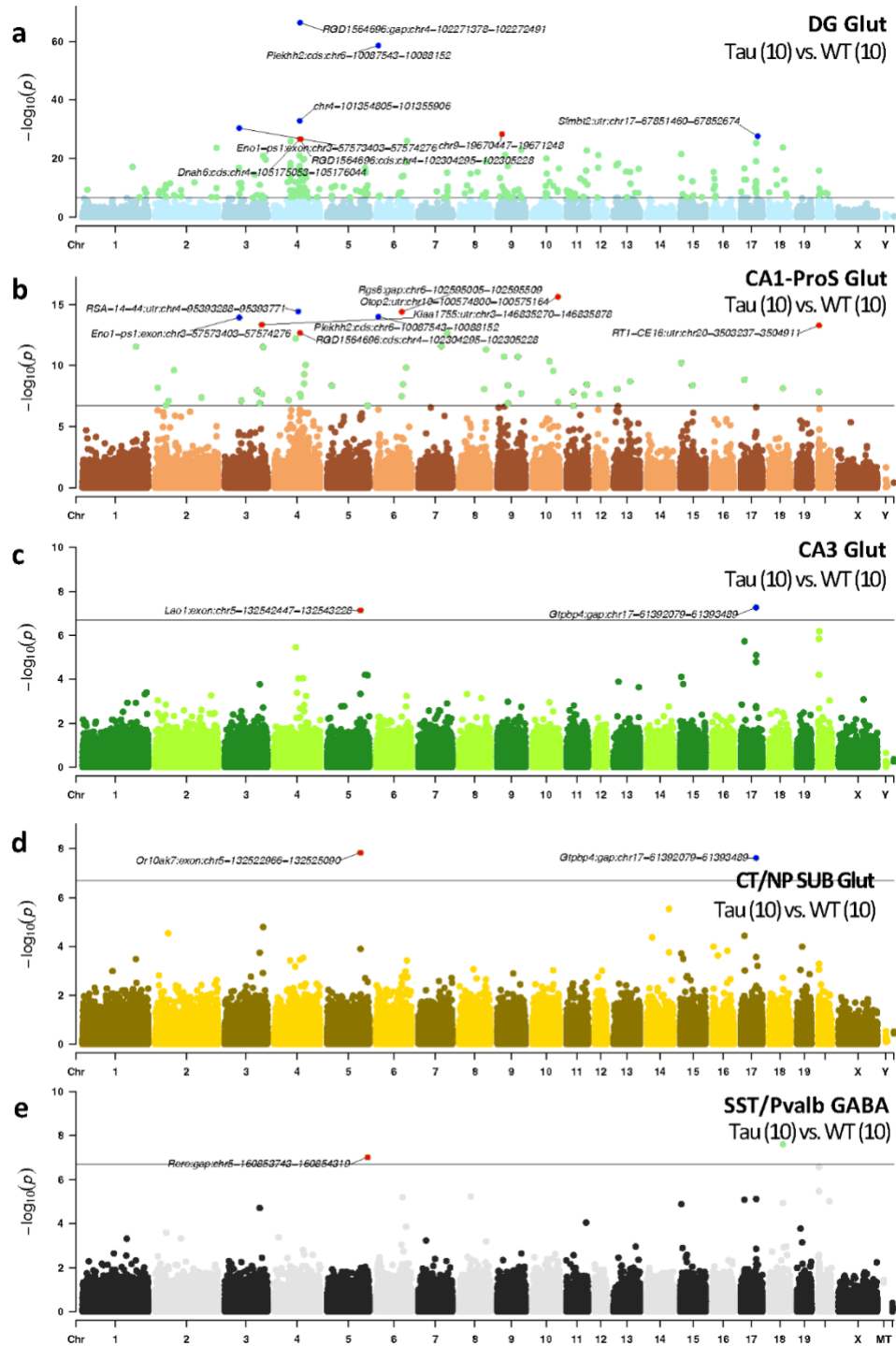
Supplementary Figure 14. Protein assessment of NTN1 and FBLN2. Capillary Western blot and quantification for NTN1 (**a,c**), and FBLN2 (**b,d**) in hippocampus of Tau-10 and WT-10. The protein of interest is boxed in red. The left panel is the protein of interest, while the right panel is the total protein. N=6-8 per group. The significance threshold was set at * <0.05 , ** <0.01 , *** <0.001 . Error bars represent SEM.



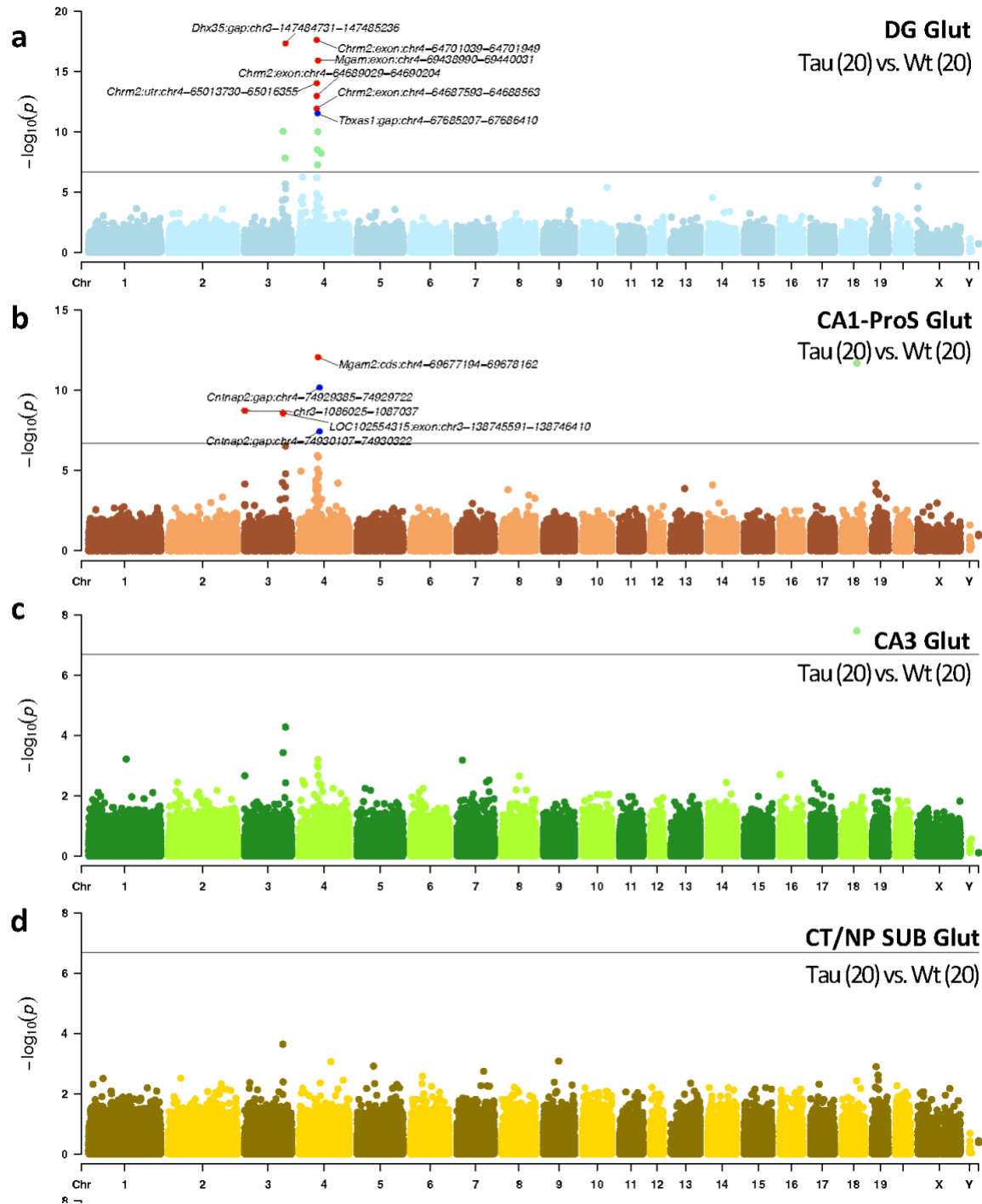
Supplementary Figure 15. Differential accessibility analysis between Tau and WT at 10 months in glial cells. Manhattan plots for astrocytes (a), oligodendrocytes (b), OPC (c), and microglia (d) show the top differential accessibility peaks in each cell type for Tau compared to WT animals at 10 months based on pseudo-bulked analysis. The black line represents the p-adjusted significance threshold. Up to 10 most significant peaks with nearby gene annotations and labelled. Blue and red dots are downregulated and upregulated in Tau compared to WT, respectively. Light green dots are other peaks that are above the significance threshold. Peaks for *Camk2a* and *Arsi* on chromosome 18 near 54300000 bp were not labelled as they are elevated due to insertion of the *hTau* transgene.



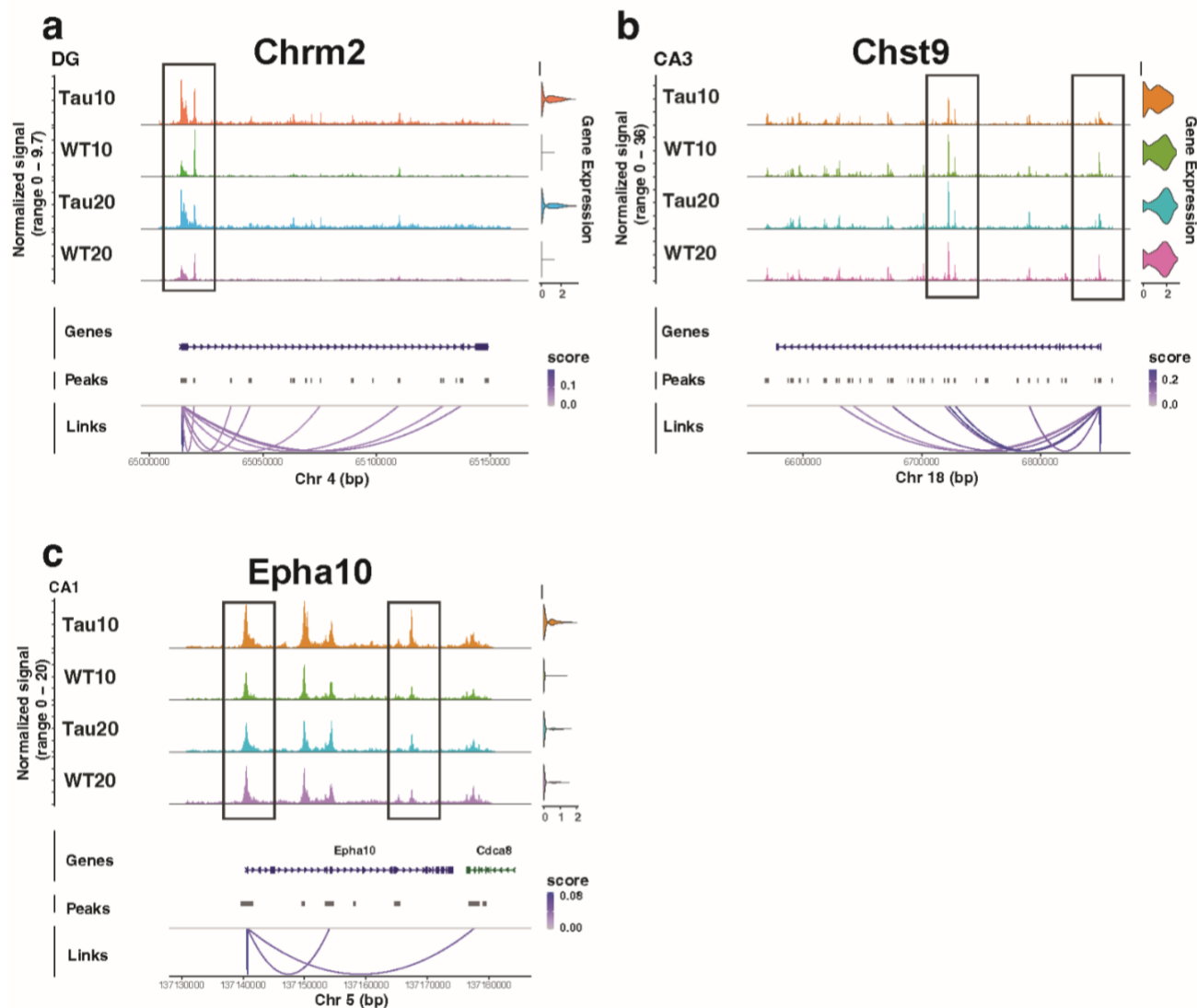
Supplementary Figure 16. Differential accessibility analysis between Tau and WT at 20 months in glial cells. Manhattan plots for astrocytes (**a**), oligodendrocytes (**b**), OPC (**c**), and microglia (**d**) show the top differential accessibility peaks in each cell type for Tau compared to WT animals at 10 months based on pseudo-bulked analysis. We observed a hotspot of differentially accessible peaks along chromosome 4 from 70000000-80000000 in oligodendrocytes (**b**). The black line represents the p-adjusted significance threshold. Up to 10 most significant peaks with nearby gene annotations and labelled. Blue and red dots are downregulated and upregulated in Tau compared to WT, respectively. Light green dots are other peaks that are above the significance threshold. Peaks for *Camk2a* and *Arsi* on chromosome 18 near 54300000 bp were not labelled as they are elevated due to insertion of the *hTau* transgene.



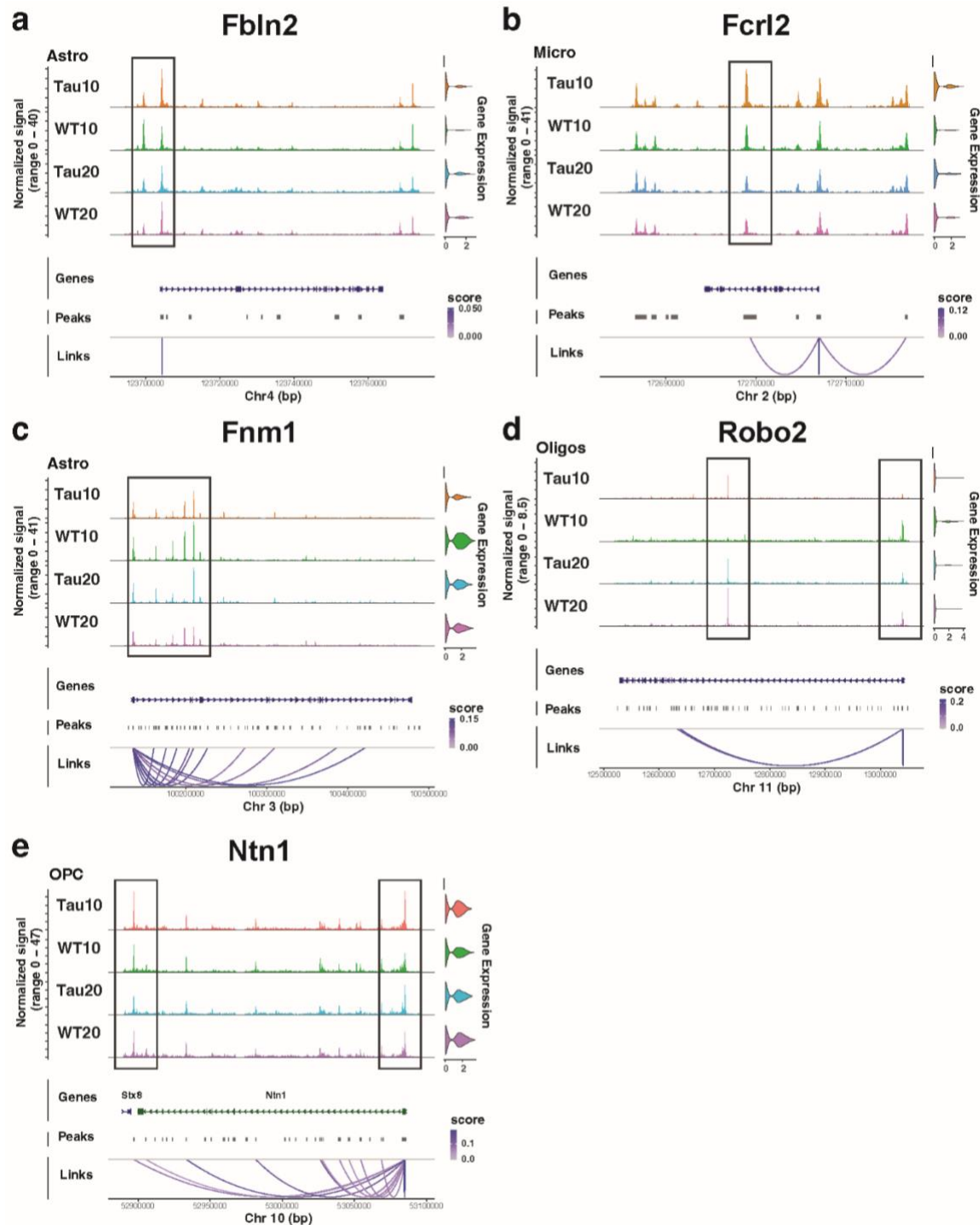
Supplementary Figure 17. Differential accessibility analysis between Tau and WT at 10 months in neuronal cells. Manhattan plots for DG Glut neurons (a), CA1-ProS Glut neurons (b), CA3 Glut neurons (c), CT/NP SUB Glut neurons (d), and SST/Pvalb GABA neurons (e) shows the top differential accessibility peaks in each cell type for Tau compared to WT animals at 10 months based on pseudo-bulked analysis. The black line represents the p-adjusted significance threshold. Up to 10 most significant peaks with nearby gene annotations and labelled. Blue and red dots are downregulated and upregulated in Tau compared to WT, respectively. Light green dots are other peaks that are above the significance threshold. Peaks for *Camk2a* and *Arsi* on chromosome 18 near 54300000 bp were not labelled as they are elevated due to insertion of the *hTau* transgene.



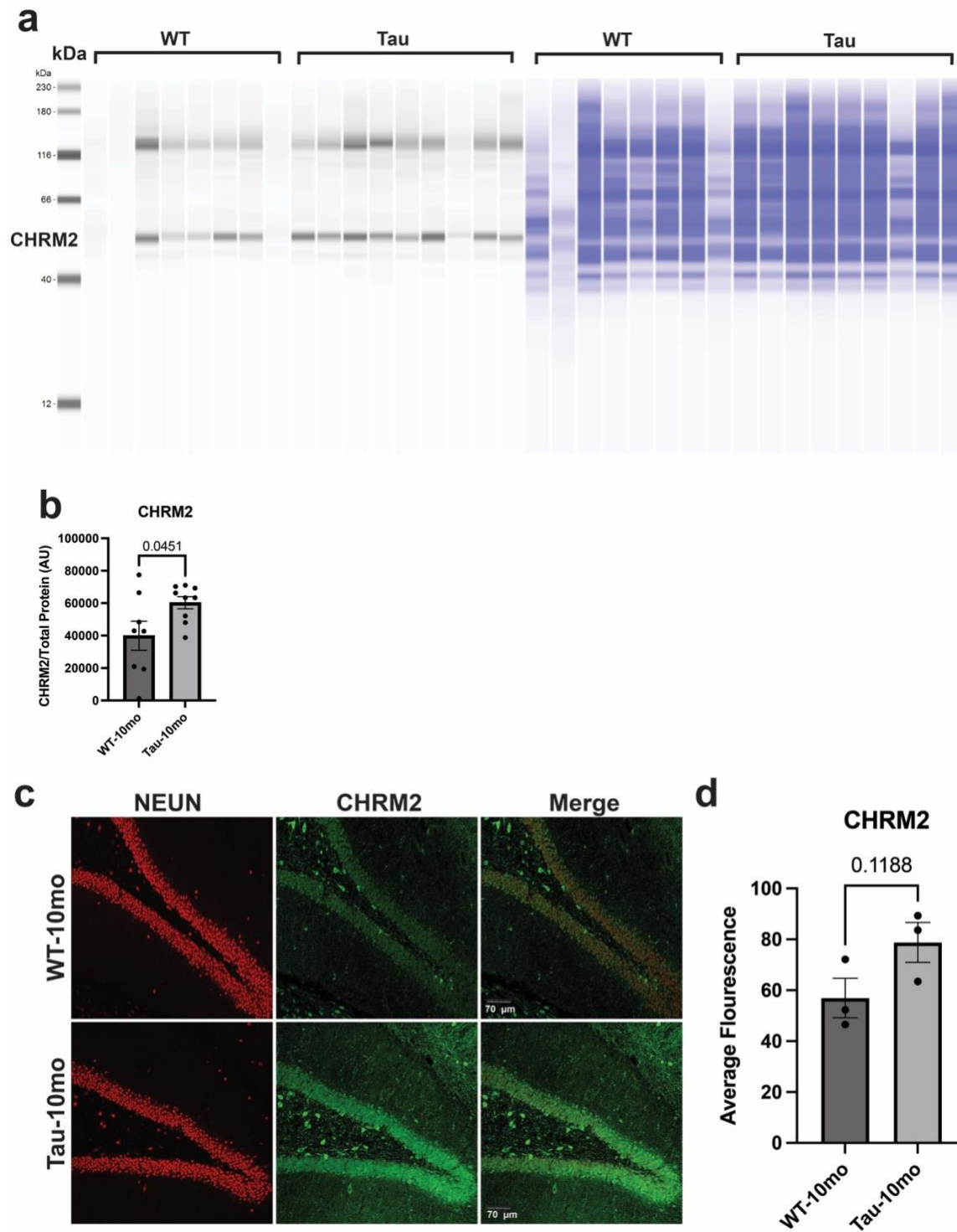
Supplementary Figure 18. Differential accessibility analysis between Tau and WT at 20 months in neuronal cells. Manhattan plots for DG Glut neurons (a), CA1-ProS Glut neurons (b), CA3 Glut neurons (c), CT/NP SUB Glut neurons (d), and SST/Pvalb GABA neurons (e) shows the top differential accessibility peaks in each cell type for Tau compared to WT animals at 10 months based on pseudo-bulked analysis. We noted a hotspot of differentially accessible peaks on chromosome 4 for both DG Glut and CA1-ProS Glut neurons. The black line represents the p-adjusted significance threshold. Up to 10 most significant peaks with nearby gene annotations and labelled. Blue and red dots are downregulated and upregulated in Tau compared to WT, respectively. Light green dots are other peaks that are above the significance threshold. Peaks for *Camk2a* and *Arsi* on chromosome 18 near 54300000 bp were not labelled as they are elevated due to insertion of the *hTau* transgene.



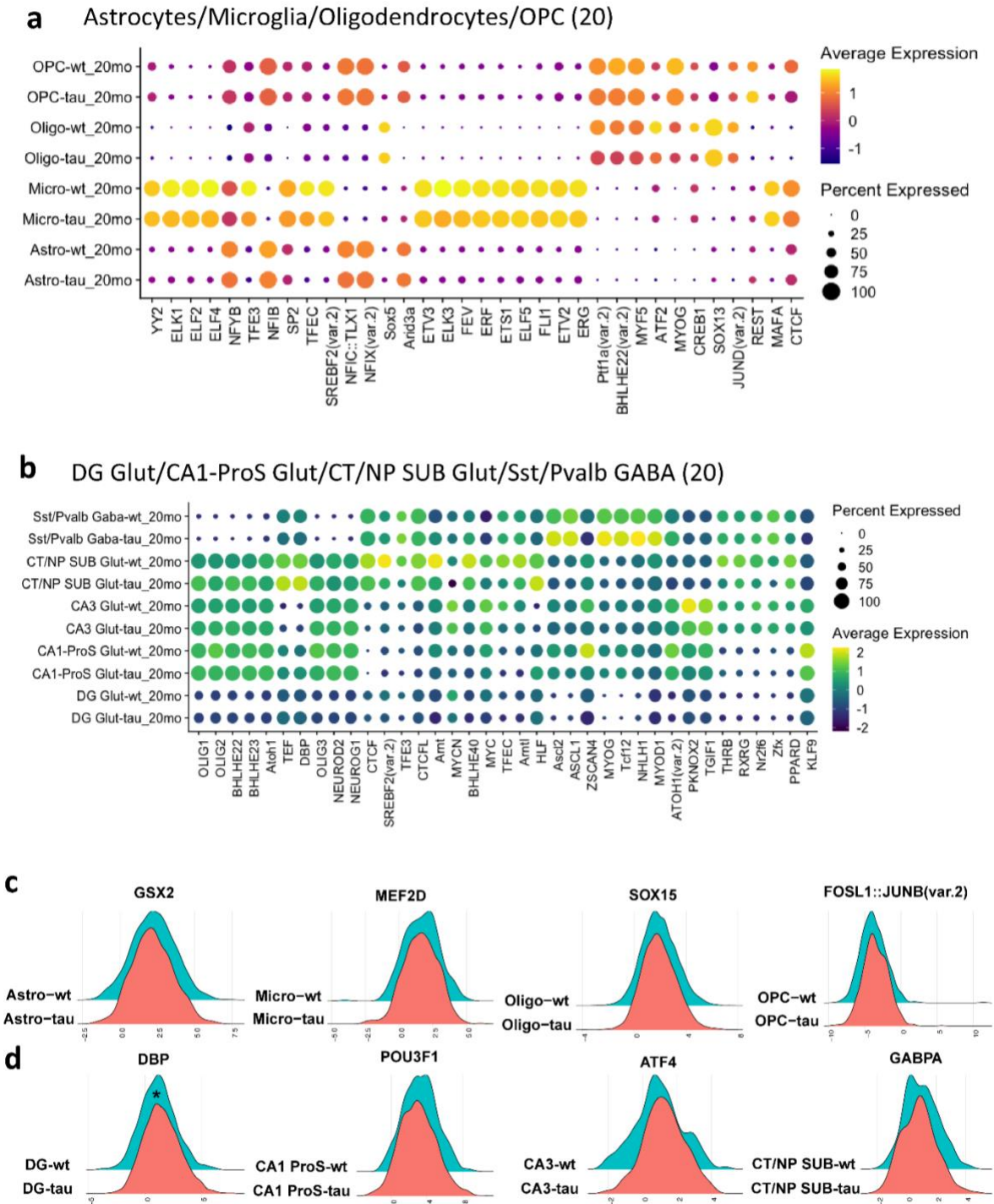
Supplementary Figure 19. ATAC signal coverage plots in glutamatergic neurons. Coverage plots created using Signac for key genes in neurons. Track shows chromatin accessibility along the chromosome by a measure of ATAC signal. **(a)** *Chrm2* in DG Glut neurons show increase in left-most peak in the box in Tau conditions, followed by decrease in right-most peak in the box with age independent of Tau or WT conditions. **(b)** *Chst9* in CA3 Glut neurons shows a decrease in Tau10 signal peaks in the left box. There was a decrease in the promoter accessibility in Tau10 and 20 compared to WT10 and 20 (shown in the right box). **(c)** *Epha10* in CA1 Glut neurons shows an increase in signal in Tau10 in both highlighted peaks. A violin plot of the gene expression is shown on the right shoulder for each gene.



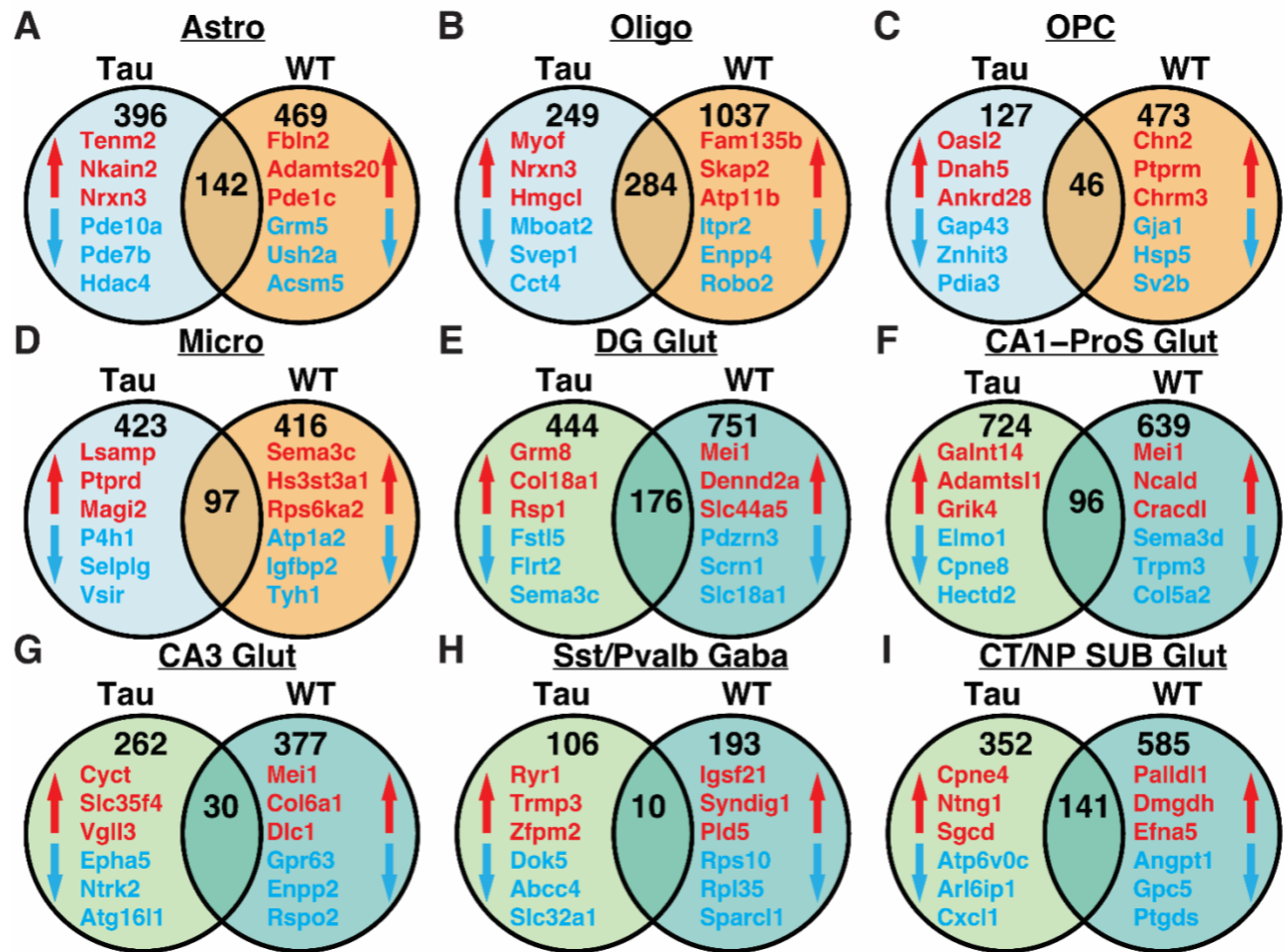
Supplementary Figure 20. ATAC signal coverage plots in glial cells. Coverage plots created using Signac for key genes in glial cell populations. Track shows chromatin accessibility along the chromosome by a measure of ATAC signal. **(a)** *Fbln2* in Astrocytes shows increase in WT10 compared to others at left-most peak in box and decrease in WT10 compared to others in right-most peak in box. **(b)** *Fcrl2* in Microglia shows an increase in Tau10 at peak in highlighted box. **(c)** *Fnm1* in Astrocytes contains multiple differential peaks highlighted in the box. WT10 appears to have the greatest signal with lower signal in other conditions and lowest in Tau20. **(d)** *Robo2* in Oligodendrocytes has decreased signal in left box and increased signal in right box for WT10. **(e)** *Ntn1* in OPC displays the greatest signal in Tau10 in both highlighted peaks. A violin plot of the gene expression is shown on the right shoulder for each gene.



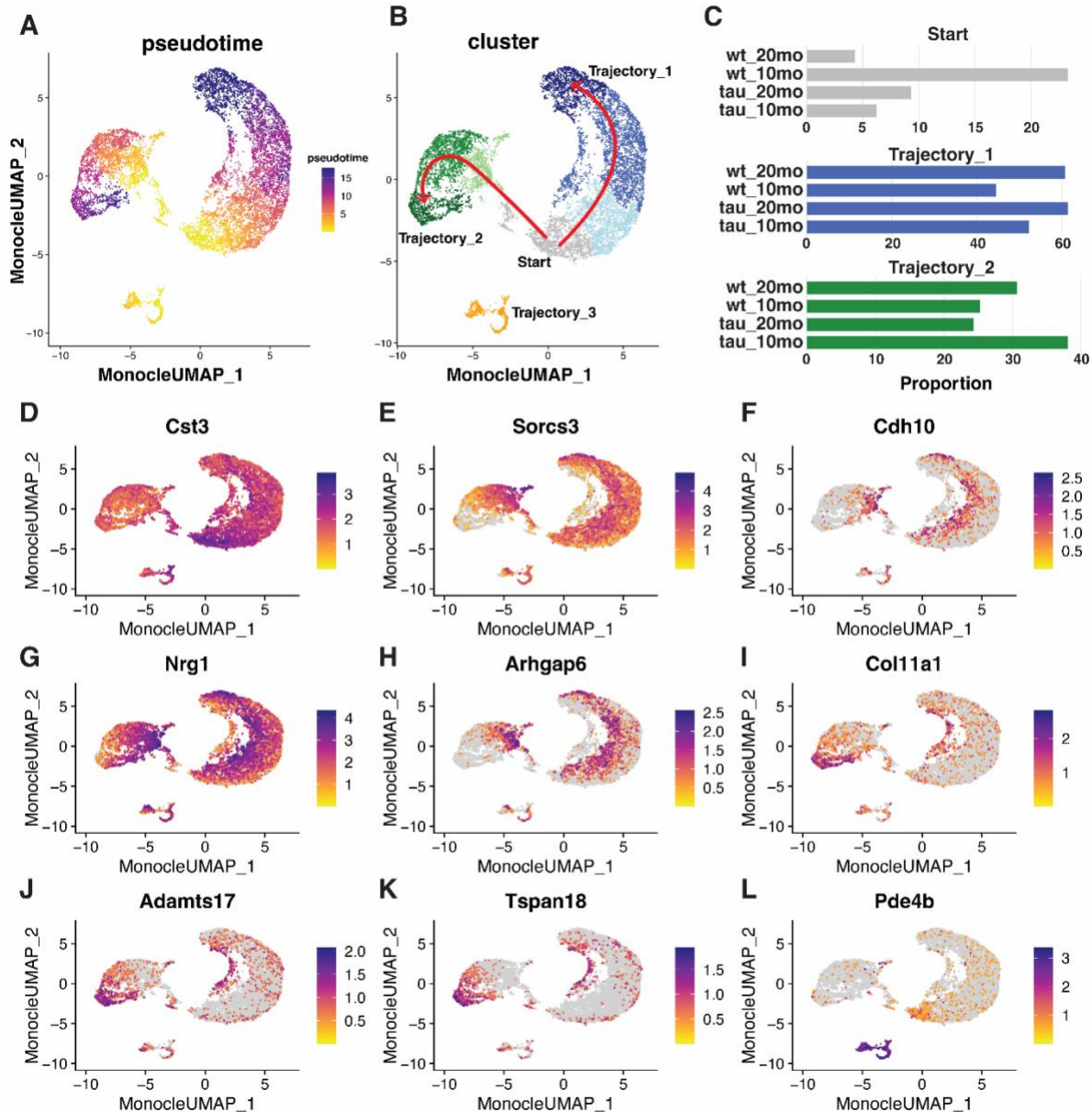
Supplementary Figure 21. Protein assessment of Chrm2. Capillary Western blot **(a)** for CHRM2 (top) and total protein (bottom). **(b)** Quantification for Chrm2 WB, N=8-9 per group. The threshold of significance was set at $p < 0.05$. **(c)** Representative immunohistochemistry (IHC) staining for CHRM2 (green), and NeuN (red) in the dentate gyrus of Tau-10 and WT-10 and accompanying quantification **(d)**. While CHRM2 was found in Tau-10 and WT-10, we observed a trend of higher average fluorescence of CHRM2 in the Tau-10. N=3b per group for IHC. Error bars represent SEM.



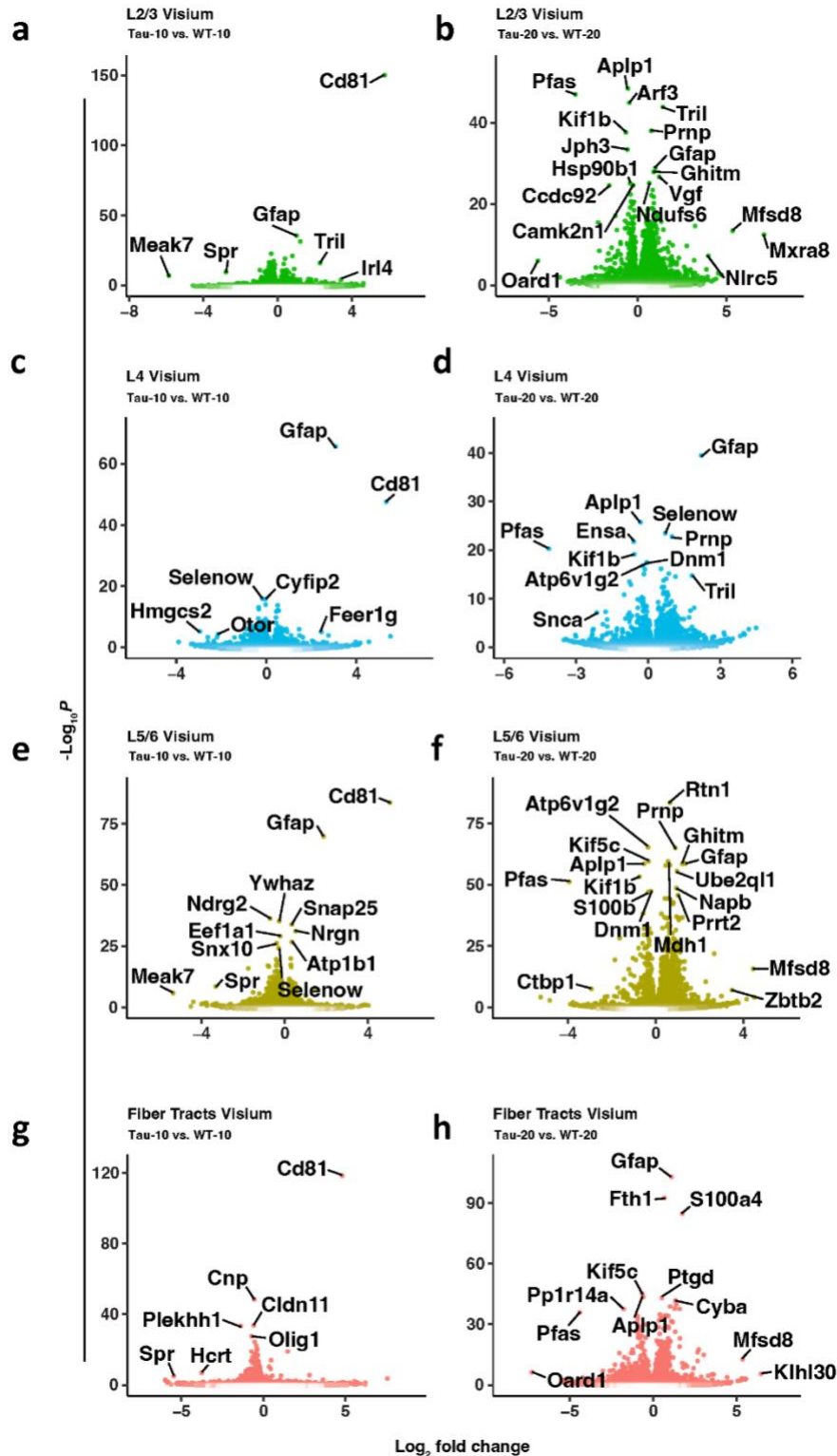
Supplementary Figure 22. Identification of putative cell-specific transcription factors differences between Tau and control at 20 months. **(a)** Enrichment of the indicated TF motifs in astrocytes, microglia, oligodendrocytes and OPC. The size of each point represents the percentage of cells expressing this motif and the color of each point represents the motif enrichment P-value ($-\log_{10}$ P-value). **(b)** TF motifs enrichment in DG Glut, CA1-ProS Glut, CA3 Glut, CT/NP SUB Glut, Sst/Pvalb Gaba neurons. The TF highlighted in the 10-mo analysis, GSX2, MEF2D, SOX15, FOSL1::JUNB(var.2), DBP, POU3F1, ATF4, and GABPA is also shown at 20-mo **(c,d)**. Only DBP was significantly increased at Tau-20 in DG Glut neurons compared to WT-20 (marked with *).



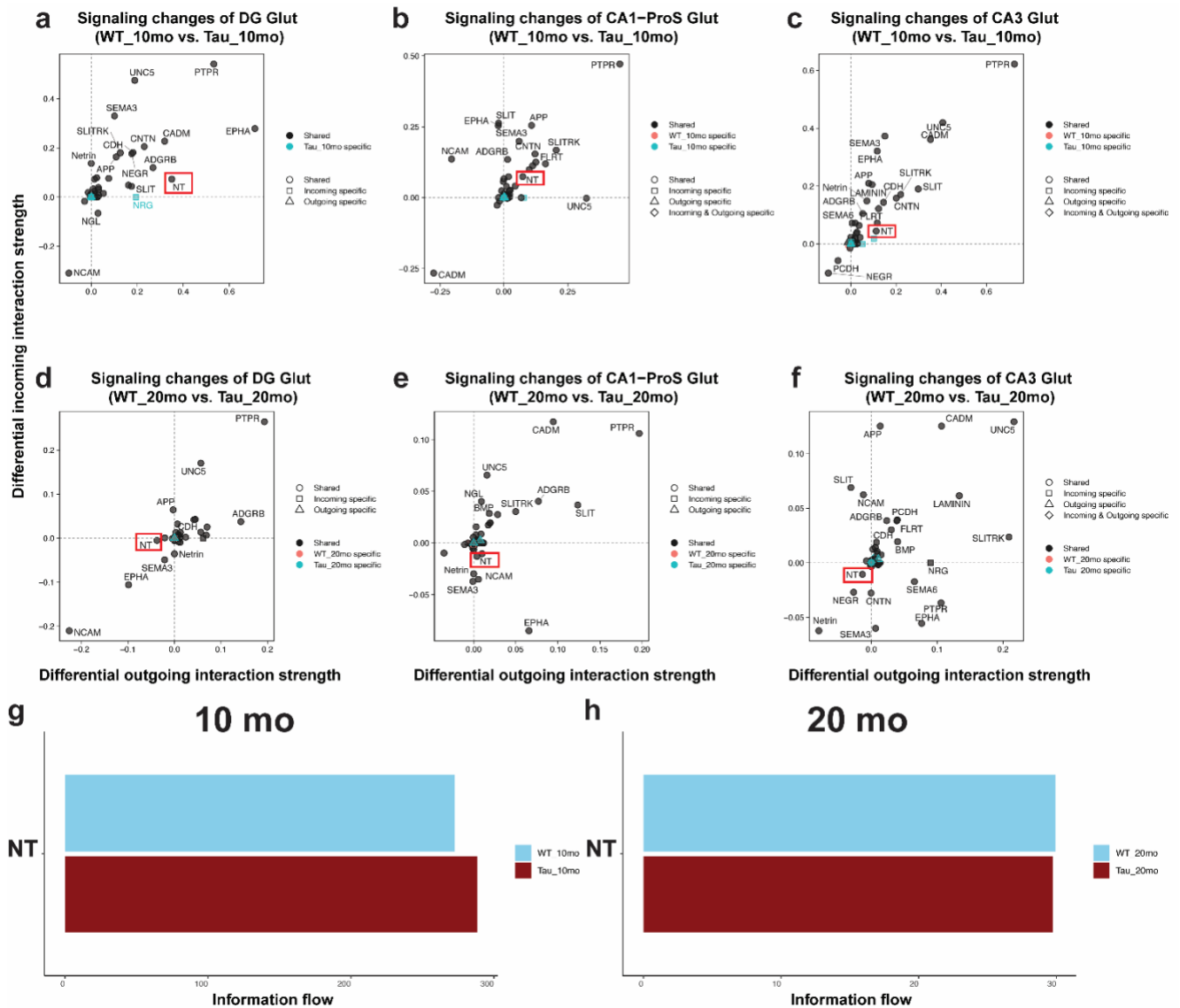
Supplementary Figure 23. Differential expression was conducted for 20 vs 10-month comparisons in each cell type for WT samples and Tau samples on filtered gene expression data. Venn diagrams shows unique differentially expressed genes in in Tau 20-mo compared to Tau 10-mo (left), common genes (middle), and unique to WT 20-mo compared to WT 10-mo (right) for the following cell types: Astro (a), Oligo (b), OPC (c), Micro (d), DG Glut (e), CA1-ProS Glut (f), CA3 Glut (g), Sst/Pvalb Gaba (h), and CT/NP SUB Glut (i). The top 3 unique gene changes that are upregulated in aging (red) and that are downregulated in aging (blue) are highlighted in each diagram. The number in each set or overlapping areas represents the total number of significant genes. DE was conducted using non-aggregated DE analysis. The full list of unique and overlapping genes are available in Supplementary Dataset 5.



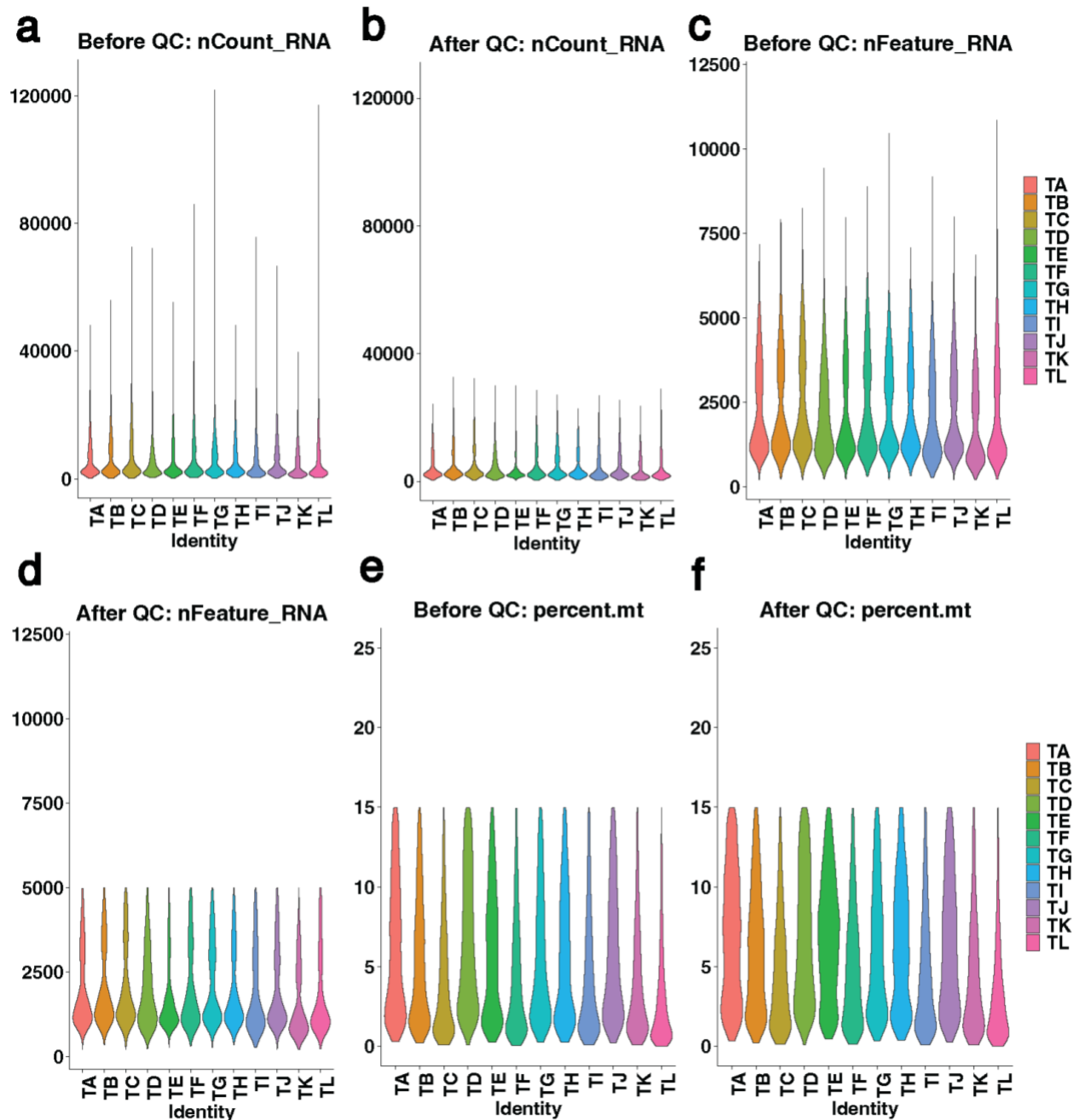
Supplementary Figure 24. Trajectory analysis of DG Glut neurons reveals dynamic cell states associated with aging and tauopathy. DG Glut neurons were subclustered and pseudo time analysis was performed using Monocle3. **(a)** Pseudo time results depict two clear trajectories. Root nodes (pseudo time = 0) were determined by locating the cluster at which there were the least aged (20-mo) neurons and highest composition of young (10-mo) neurons to simulate aging along the trajectory. **(b)** Clustering results and annotation along the separate trajectories to highlight the directionality of cell state changes. Representative arrows depict directionality along two main trajectories. **(c)** Bar plots displaying proportion of cells within each condition that are present at the start, along trajectory 1, and along trajectory 2. The origin cluster is favored by WT 10-mo DG Glut neurons as expected, as the trajectory highlights aging. However, the lack of Tau 10-mo DG Glut neurons at the origin indicates potential early aging cell state. Trajectory 1 appears to display normal aging as both WT 20-mo and Tau 20-mo neurons are favored over 10 mo. Trajectory 2 appears to be favored only by Tau 10-mo neurons, indicating a potential disease or dysfunctional state. The main marker for the start cluster was Cst3 **(d)**. The main markers for trajectory 1 were Sorcs3 **(e)**, Cdh10 **(f)**, Nrg1 **(g)**, and Arhgap6 **(h)**. The main markers for trajectory 2 were Col11a1 **(i)**, Adamts17 **(j)**, and Tspan18 **(k)**. Additionally, a small cluster was found and labeled trajectory 3. The top gene marker for this cluster was Pde4b **(l)**, but due to low cell count, the cluster was not analyzed further.



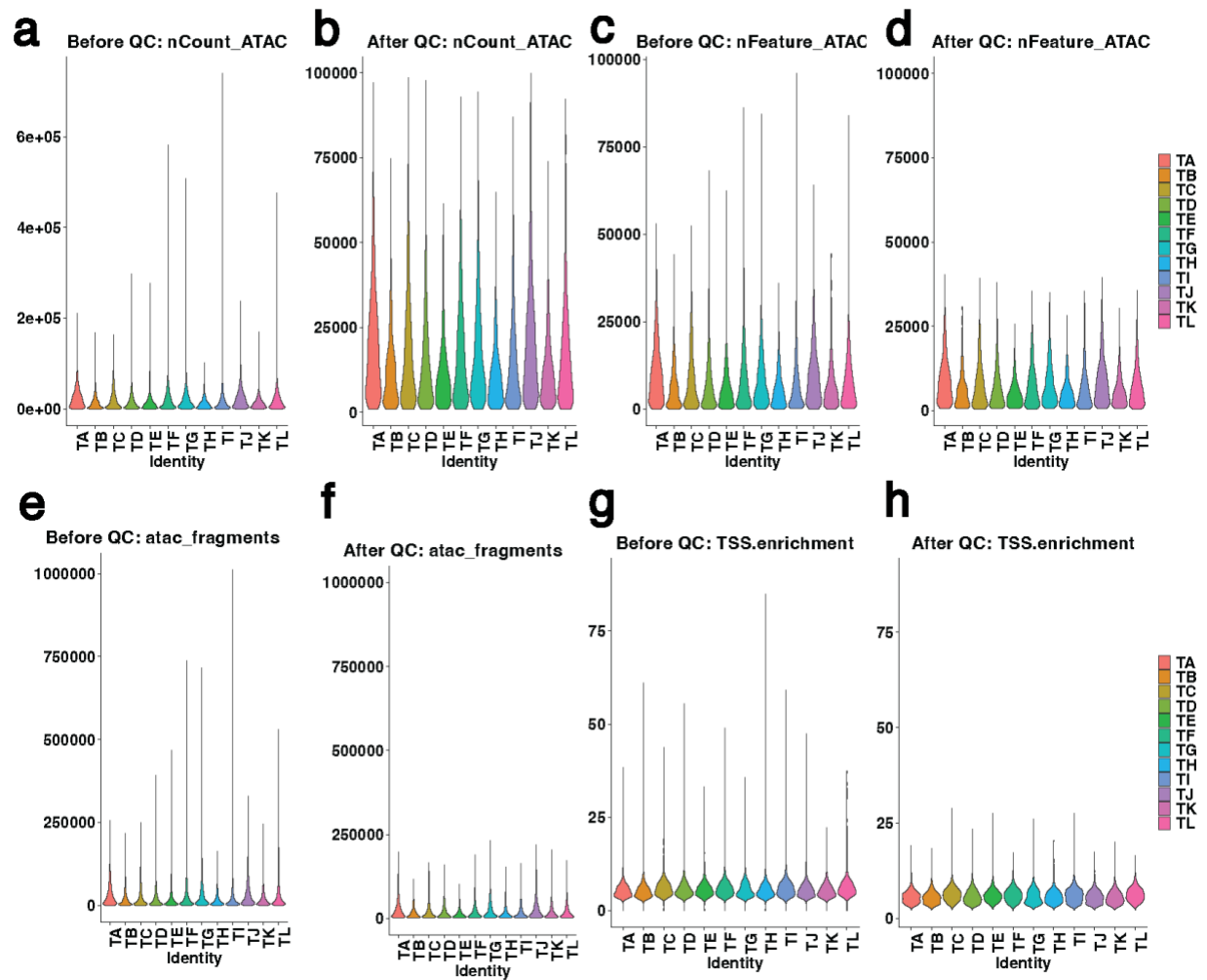
Supplementary Figure 25. Additional 10x Visium DEG analysis comparing non-hippocampal regions between Tau and WT at 10 and 20 months. Volcano plots of Tau vs. WT 10 and 20-month differential abundance analysis for the L2/3 cortex (**a,b**), L4 cortex (**c,d**), L5/6 cortex (**e,f**), and Fiber tracts (**g,h**) with the log₂ fold changes on the X-axis. P-values ($-\log_{10}$ P-value) are plotted on the Y-axis. Labelled genes have p-adjusted < 0.05.



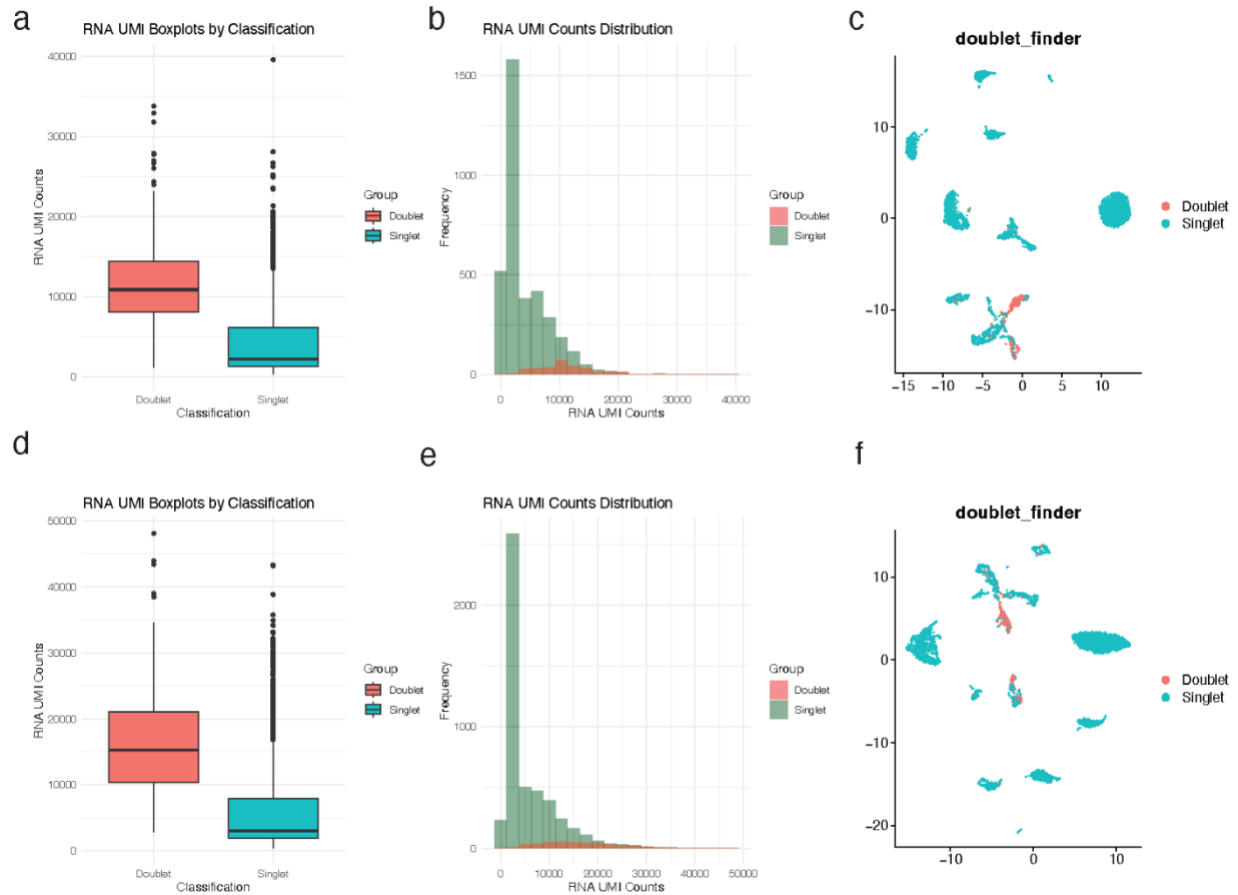
Supplementary Figure 26. CellChat analysis of the Neurotrophin (NT) communication network using the snRNA data. (a-f) Differential signaling strength comparison of Tau and WT at 10-mo and 20-mo in DG Glut, CA1-ProS Glut, and CA3 Glut neurons. NT signaling is boxed in red. There was no substantial change in any of the cell types for NT signaling. The total NT signaling strength was comparable between Tau and WT at 10-mo (g), and 20-mo (h).



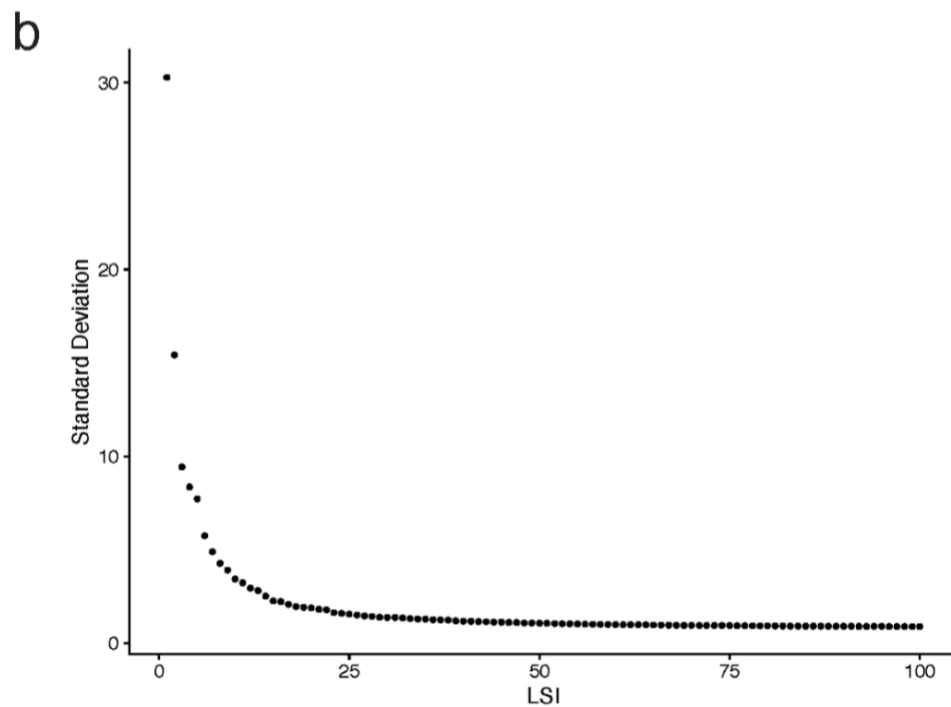
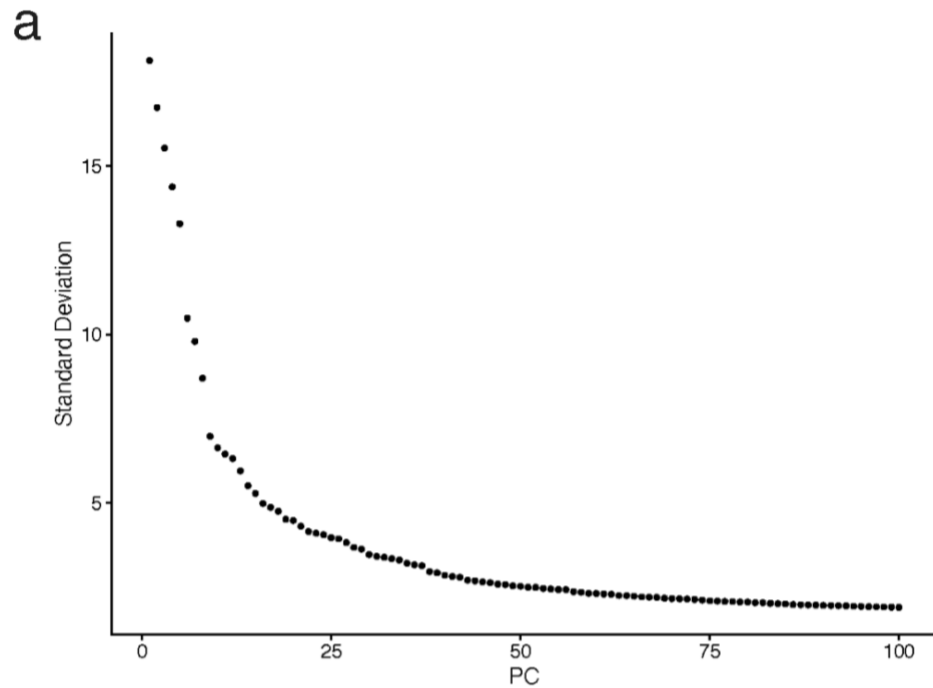
Supplementary Figure 27. Quality Control for snRNA. Per nuclei distribution for the following metrics are shown before and after QC filtering: (a,b) total RNA count, (c,d) number of genes, (e,f) percentage of mitochondrial genes. The sample coding are as follows: Tau-10mo (TA, TB, TC), WT-10mo (TD, TE, TF), Tau-20mo (TG, TH, TI), and WT-20mo (TJ, TK, TL).



Supplementary Figure 28. Quality Control for snATAC. Per nuclei distribution for the following metrics are shown before and after QC filtering: **(a,b)** total ATAC count, **(c,d)** number of unique ATAC features, **(e,f)** total ATAC fragment count, **(g,h)** Transcription start site (TSS) enrichment score. The sample coding are as follows: Tau-10mo (TA, TB, TC), WT-10mo (TD, TE, TF), Tau-20mo (TG, TH, TI), and WT-20mo (TJ, TK, TL).



Supplementary Figure 29. Quality Control using Doublet Finder. Doublet Finder was performed on a per-sample basis to identify and exclude predicted multiplets as part of QC filtering. The doublet outputs from two samples are shown (a-f). We saw predicted doublets having higher average counts of RNA UMI (a,d) and forming the right tail of the histogram (b,f). Furthermore, doublets tended to cluster together (c,f) in dimensional reduction plots.



Supplementary Figure 30. Principal Component and Latent Semantic Analysis for RNA and ATAC clustering. Elbow plot showing Standard Deviations of each principal component from PCA analysis on RNA data (**a**). Elbow plot showing Standard Deviation of each principal component from LSI analysis on ATAC data (**b**). The first LSI component had a high degree of correlation with sequencing depths and was not used for clustering.

Supplementary Tables

ID	Age (months)	Sex	Genotype	Experiment
6188	10	M	-/-	WB
6198	10	M	-/-	WB
6204	10	F	-/-	WB
6233	10	F	+/+	WB
6237	10	F	+/+	WB
6238	10	F	+/+	WB
8186	10	F	+/+	WB
8187	10	F	+/+	WB
8188	10	F	+/+	WB
8196	10	F	-/-	WB
8199	10	F	-/-	WB
8200	10	F	-/-	WB
8730	10	F	+/+	WB
8732	10	F	-/-	WB
8738	10	M	+/+	WB
8743	10	M	+/+	WB
8757	10	F	-/-	WB
8293	20	F	-/-	Visium
8294	20	F	+/+	Visium
8543	10	M	-/-	Visium
8546	10	F	+/+	Visium
6439	20	F	+/+	Single-Cell Multiome
6520	20	F	+/+	Single-Cell Multiome
6522	20	F	-/-	Single-Cell Multiome
6532	20	F	-/-	Single-Cell Multiome
6548	20	F	-/-	Single-Cell Multiome
6553	20	F	+/+	Single-Cell Multiome
8186	10	F	+/+	Single-Cell Multiome
8187	10	F	+/+	Single-Cell Multiome
8188	10	F	+/+	Single-Cell Multiome
8196	10	F	-/-	Single-Cell Multiome
8199	10	F	-/-	Single-Cell Multiome
8200	10	F	-/-	Single-Cell Multiome
6188	10	M	-/-	IHC
6198	10	M	-/-	IHC
6204	10	F	-/-	IHC
6212	10	F	+/+	IHC
6233	10	F	+/+	IHC
6237	10	F	+/+	IHC

Supplementary Table 1. List of the ID, Age, Sex, Genotype (+/+ are the McGill-R955-hTau transgenic rats and -/- are the WT controls), and the experiment each rat was part of. We did not implement any exclusion criteria for the experimental animals.

Antigen	Abbreviation	Species reactivity	Dilution	Source
Muscarinic Acetylcholine Receptor M2	Chrm2	Human, Mouse, Rat	1/100 IHC, 1/50 WB	Novus Biologicals, part of Bio-Techne, Minneapolis, MN, Catalog # NBP3-16576
Neuronal nuclei	NeuN	Human, Mouse, Rat	1/500 IHC	Cell Signaling Technology, Danvers, MA, Catalog # 94403
Fibulin 2	Fbln2	Human, Mouse, Rat	1/50 WB	Thermo Fisher Scientific, Waltham, MA, Catalog # PA5-21640
Netrin 1	Ntn1	Human, Mouse, Rat	1/50 WB	Proteintech, Rosemont, IL, Catalog # 20235-1-AP

Supplementary Table 2. List of antibodies used for Western blot and immunohistochemistry (IHC) analyses. The table includes the antibody name, source, catalog number, dilution factor, and the specific application (Western blot or IHC).

